



**Journal of
Mechanics of
Materials and Structures**

**CONJUGATE STRESS/STRAIN BASE PAIRS FOR
PLANAR ANALYSIS OF BIOLOGICAL TISSUES**

Alan D. Freed, Veysel Erel and Michael R. Moreno

Volume 12, No. 2

March 2017



CONJUGATE STRESS/STRAIN BASE PAIRS FOR PLANAR ANALYSIS OF BIOLOGICAL TISSUES

ALAN D. FREED, VEYSEL EREL AND MICHAEL R. MORENO

A theoretical framework is presented for the analysis of planar membranes based upon a triangular (as opposed to a polar) decomposition of the deformation gradient. This leads to a distillation of the deformation gradient into three distinct modes. Each mode can, in principle, be individually activated in an experiment. Measures of stress are shown to exist for each mode of strain so that the stress power can be decomposed into independent additive parts. The outcome is a set of three conjugate stress/strain base pairs (each being a pair of scalars) from which constitutive equations can be constructed for planar solids without relying on tensor invariants to cast the theory. Explicit and implicit elastic models are derived that, when convolved, produce a material model whose stress/strain response is indicative of soft biological tissues. Stress/strain curves for each conjugate pairing are constructed from published experimental data. The model describes these data.

1. Introduction

Recent advances in regenerative medicine include the ability to tune the mechanical properties of engineered tissue constructs, e.g., [Amensag and McFetridge 2014; Kharaziha et al. 2013; Xie et al. 2015]. With the advent of this capability, the challenges have become these: what mechanical properties have relevance when designing a tissue-engineered construct? What should the target values for these mechanical properties be? Ideally, an engineered tissue graft, say, would possess the same mechanical properties as the native tissue, and integrate seamlessly with respect to mechanical performance. Most efforts to characterize the mechanical properties of tissue-engineered constructs have been based on numerous simplifying assumptions (linear, homogeneous, isotropic) that typically treat the engineered construct as a linear elastic material. These assumptions enable uniaxial mechanical tests to be conducted wherein, e.g., a quasielastic modulus and a tensile strength can be determined. Unfortunately, this form of mechanical characterization is ineffective at providing insight into how well an engineered tissue actually mimics the native tissue *in vivo*. Biological tissues are complex materials that typically undergo large deformations. They also exhibit complex mechanical behaviors that likely include a nonlinear stress/strain curve, mechanical anisotropy, and a viscoelastic response.

The utility of treating an engineered tissue construct as a linear elastic material when establishing mechanical properties is that it enables one-to-one comparisons between materials. A quasimodulus and the tensile strength are physical parameters, each corresponding with a specific measurable physical property; however, the quasimodulus lacks uniqueness. The issue is this: soft tissues are not linear elastic.

Veysel Erel received financial support from the Ministry of National Education, Turkey. Michael R. Moreno received financial support from an NSF GOALI award.

Keywords: thermodynamic conjugate pairs, distortion, Gram–Schmidt decomposition, membrane, soft tissues.

To address this nonlinearity, Fung [1993, §7.12] proposed an exponential strain-energy function of the form

$$W = \frac{1}{2}(q + c(e^Q - 1)),$$

whose parameters q and Q are quadratic forms in strain described by

$$q = a_{ijkl} E_{ij} E_{kl} \quad \text{and} \quad Q = b_{ijkl} E_{ij} E_{kl},$$

with E_{ij} denoting strain components evaluated in a Lagrangian coordinate frame. There are nine constants to parameterize for the planar case: c , four a_{ijkl} and four b_{ijkl} , because $a_{ijkl} = a_{klij}$ and $b_{ijkl} = b_{klij}$ with $i, j = 1, 2$. Unfortunately, in this framework, there is no analog to an elastic modulus, i.e., there is no parameter that corresponds with some unique, measurable, mechanical property. This system of equations is indeterminable. In practice, data is gathered and a nonlinear least squares fit is used to “solve” the system. Numerous combinations of constants (a_{ijkl} , b_{ijkl} , c) usually exist, each representing a reasonable mathematical solution. Even though these parameters have utility in their ability to fit a curve to the data, they (unfortunately) cannot be compared between fits of different materials or samples because the model parameters themselves lack uniqueness and physical interpretation.

This unintended side effect of the Fung approach compromises its utility for the practical purpose of designing engineered tissues with the intent of mimicking Mother Nature. Without unique and physical material parameters, it is difficult to use such an approach for engineering synthesis, which is evident in the apparent absence of models like Fung’s in the tissue engineering literature. This fundamental need of the practicing tissue engineer motivated our study.

We seek a material model for planar membranes whose parameters are true material constants in that their values are unique, physical and readily extracted from stress/strain curves. Future work will focus on applying our model to tissue engineering. Here we focus on deriving the model.

The methodology developed herein leads to a material model described by three distinct stress/strain curves. Each unique curve is characterized by three parameters. So our model and Fung’s model are both described in terms of nine parameters. The difference being that our model is comprised of three uncoupled responses, a response for each conjugate pairing, with data from each mode having sensitivity to its three independent parameters. Whereas, Fung’s model, e.g., is described over the whole of two-space wherein all nine parameters must be fit simultaneously, and getting a data set that is rich enough to secure parameter sensitivity to all of its model parameters is problematic at best. The presumed independence of the thermodynamic conjugate pairs in our approach greatly facilitates parameterization of our model. The theory derived in this paper does not follow a conventional approach, viz., it is not constructed from invariant theory; rather, it is founded upon the following conjecture.

Hypothesis. The governing tensors for stress and the rate of deformation can be encoded into a set of independent conjugate base pairs wherein each stress/strain conjugate pair is a scalar pair. Individual constitutive equations govern the response of each base pair, which may be elastic, viscoelastic, etc., as determined from experiment. After the separate constitutive equations for all base pairs have been solved, their constituents can be decoded to update the tensorial states of stress and the rate of deformation. An admissible encoding/decoding algorithm is one-to-one.

The paper begins with a discussion of kinematics, including a discussion of the difference between three frames of reference that are used: the Lagrangian frame, a material frame, and the Eulerian frame.

In this material frame, work can be decomposed into three parts: dilation, squeeze and shear. From here it is possible to extract three conjugate stress/strain pairs, one describing each deformation mode. They are generalized displacements and tractions in the terminology of Hill [1978]. An encoding/decoding algorithm is put forward that maps tensor components into conjugate base pairs and then back again. The thermodynamic couplings of Kelvin and Poynting are addressed. Explicit and implicit elastic solids are derived for planar membranes that, when convolved, transform into a constitutive theory that is suitable for describing soft biological tissues. The model is demonstrated by fitting it to experimental data taken from the literature.

There are five appendices. The first two compare the polar and triangular decompositions of the deformation gradient for planar deformations. The third addresses acquisition of the components for deformation and stress from planar experiments. The fourth derives stress power in terms of the triangular decomposition. And the fifth decomposes the triangular description for deformation into three distinct modes: dilation, squeeze and shear.

2. Kinematics

A theoretical framework is presented in this document for the analysis of materials that are planar sheets whose utility is expected to reside in engineering design and synthesis. Experiments done on planar membranes have a long history in the biomechanics literature, primarily studied for the purpose of parameterizing material models [Grashow et al. 2006; Humphrey et al. 1987; Lanir and Fung 1974; Sacks 1999; 2000; Sacks and Chuong 1993]. It is assumed that extensions and tractions are determined, to sufficient accuracy, by the deformation of the middle surface of a sheet and, as such, the theory can be cast in \mathbb{R}^2 . Membrane thickness need not enter into the construction. Influences arising from membrane curvature [Evans and Skalak 1979; Helfrich 1973; Humphrey 1998] are neglected because the radii of curvature are taken to be infinite. For the interested, tension-field theory [Pipkin 1986; Steigmann 1990] should be a viable approach to handle wrinkling, which is not addressed herein.

A material particle of interest is located at position \mathbf{X} in a reference state at time t_0 that at current time t is located by a different position vector \mathbf{x} . The motion of this particle is described by a vector function $\mathbf{x} = \boldsymbol{\chi}(\mathbf{X}, t)$ that is invertible in the sense that a complementary vector function $\mathbf{X} = \boldsymbol{\chi}^{-1}(\mathbf{x}, t)$ exists so that $\mathbf{X} = \boldsymbol{\chi}^{-1}(\boldsymbol{\chi}(\mathbf{X}, t), t)$ [Truesdell and Noll 2004]. Motions are considered to be sufficiently smooth so that the required derivatives exist. A particle traverses its path of motion $\boldsymbol{\chi}$ through space with a velocity of $\mathbf{v} = \partial \boldsymbol{\chi}(\mathbf{X}, t) / \partial t = \dot{\mathbf{x}}$.

An areal element dA of infinitesimal extent within a planar membrane consists of a dense set of point particles filling a connected region in \mathbb{R}^2 at time t_0 . This same collection of material particles corresponds with another areal element da at time t . From the conservation of mass comes $dm = \rho_0 dA = \rho da$. This areal element has a fixed mass of dm with planar densities $\rho_0 = dm/dA$ and $\rho = dm/da$ at times t_0 and t , and is considered to undergo affine motions.

Deformation at a particle is described by the gradient of its motion $\boldsymbol{\chi}$ taken with respect to its position \mathbf{X} that produces a two-point tensor field \mathbf{F} described by

$$\mathbf{F} = \frac{\partial \boldsymbol{\chi}(\mathbf{X}, t)}{\partial \mathbf{X}}, \quad \text{which is commonly written as} \quad \mathbf{F} = \frac{\partial \mathbf{x}}{\partial \mathbf{X}}. \quad (1a)$$

Its inverse \mathbf{F}^{-1} exists because the Jacobian of deformation $J := \det \mathbf{F} = da/dA = \rho_0/\rho$ must be positive from the conservation of mass, thereby allowing one to write

$$\mathbf{F}^{-1} = \frac{\partial \mathbf{X}^{-1}(\mathbf{x}, t)}{\partial \mathbf{x}}, \quad \text{which is commonly written as} \quad \mathbf{F}^{-1} = \frac{\partial \mathbf{X}}{\partial \mathbf{x}}. \quad (1b)$$

The deformation gradient is a linear transformation that maps tangent vectors between the current (Eulerian) and reference (Lagrangian) configurations with a push-forward map of $d\mathbf{x} = \mathbf{F} d\mathbf{X}$ and a pull-back map of $d\mathbf{X} = \mathbf{F}^{-1} d\mathbf{x}$. Symmetric and upper-triangular decompositions of the deformation gradient and its inverse are presented in Appendix A and Appendix B for the case of planar membranes.

3. Base vectors

At this point in our development we deviate from the path normally followed by decomposing the deformation gradient \mathbf{F} into a product between an orthogonal rotation \mathbf{Q} and an upper-triangular distortion $\tilde{\mathbf{F}}$, see Appendix B, instead of as a product between another orthogonal tensor \mathbf{R} ($\neq \mathbf{Q}$) and a symmetric stretch \mathbf{U} , see Appendix A. Specifically, we adopt a \mathbf{QR} (Gram–Schmidt) decomposition of \mathbf{F} introduced into the mechanics literature by Srinivasa [2012] who expressed it as $\mathbf{F} = \mathbf{Q}\tilde{\mathbf{F}}$.¹ He explored using this decomposition in lieu of adopting the polar decomposition $\mathbf{F} = \mathbf{R}\mathbf{U}$ used throughout mechanics. Rosakis [1990] also derived an upper-triangular decomposition for the deformation gradient by considering materials with a preferred material orientation, his interests being phase transformations and twinning in crystals. He did not use the \mathbf{QR} matrix decomposition from linear algebra in his kinematic analysis. Freed and Srinivasa [2015] derived the components for $\ln \tilde{\mathbf{F}}$, considering its applicability as a strain measure, and have studied $\tilde{\mathbf{F}}$ for a variety of boundary value problems used in material characterization.

There are three sets of orthogonal base vectors to sort out when using this approach for kinematic analysis, as depicted in Figure 1. They are rectangular Cartesian coordinate frames. There is a natural set of Lagrangian base vectors $\{\mathbf{n}_1, \mathbf{n}_2\}$. The Lagrangian base vectors rotate from an Eulerian frame $\{\mathbf{e}_1, \mathbf{e}_2\}$ via an orthogonal matrix $[\mathbf{R}]$ that comes from the polar decomposition of \mathbf{F} , viz., $\mathbf{F} = \mathbf{R}\mathbf{U}$. The Eulerian frame is typically considered to be fixed in space, e.g., a coordinate frame in one’s laboratory, through which the body translates, rotates and deforms over time. There is also a set of material base vectors $\{\mathbf{m}_1, \mathbf{m}_2\}$ that rotate from the Eulerian frame via an orthogonal matrix $[\mathbf{Q}]$ that comes from the \mathbf{QR} decomposition of \mathbf{F} , viz., $\mathbf{F} = \mathbf{Q}\tilde{\mathbf{F}}$. In the material frame $\{\mathbf{m}_1, \mathbf{m}_2\}$, direction \mathbf{m}_1 remains tangent to a physical material line at the coordinate origin [Srinivasa 2012]. Maps between the three sets of base vectors obey

$$\mathbf{m}_\xi = \mathbf{e}_i Q_\xi^i, \quad (2a)$$

$$\mathbf{n}_I = \mathbf{e}_i R_I^i, \quad (2b)$$

$$\mathbf{n}_I = \mathbf{m}_\xi \tilde{R}_I^\xi = \mathbf{m}_\xi [Q^{-1}]_i^\xi R_I^i, \quad (2c)$$

and therefore $\tilde{\mathbf{R}} := \mathbf{Q}^T \mathbf{R}$, as drawn in Figure 1. Here lower-case Latin indices associate with the Eulerian frame $\{\mathbf{e}_1, \mathbf{e}_2\}$, upper-case Latin indices associate with the Lagrangian frame $\{\mathbf{n}_1, \mathbf{n}_2\}$, Greek indices

¹ Notation $\mathbf{Q}\tilde{\mathbf{F}}$ is chosen over notation \mathbf{QR} because \mathbf{R} is commonly used in the polar decomposition of the deformation gradient to denote its rotational component, whereas, in the mathematics literature \mathbf{R} in \mathbf{QR} denotes a right-triangular matrix that we call distortion. Srinivasa [2012] introduced his notation to avoid potential confusion within the mechanics community.

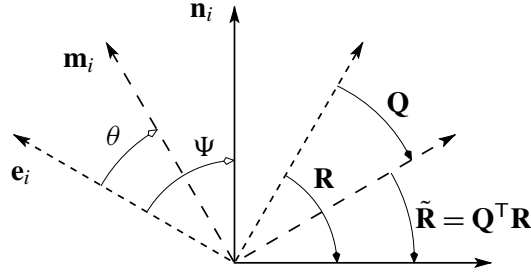


Figure 1. The Lagrangian (natural) base vectors \mathbf{n}_i are located by a rotation \mathbf{R} through an angle ψ measured from an Eulerian coordinate frame with base vectors \mathbf{e}_i , therefore $\mathbf{n}_i = \mathbf{e}_i \mathbf{R}$, where $i = 1, 2$. Rotation \mathbf{R} is established through a polar decomposition of the deformation gradient $\mathbf{F} = \mathbf{R}\mathbf{U}$. Similarly, the material base vectors \mathbf{m}_i are located by a rotation \mathbf{Q} through an angle θ measured from the Eulerian base vectors \mathbf{e}_i , hence $\mathbf{m}_i = \mathbf{e}_i \mathbf{Q}$. Rotation \mathbf{Q} is established through a triangular decomposition of the deformation gradient $\mathbf{F} = \mathbf{Q}\tilde{\mathbf{F}}$. The Lagrangian frame $\{\mathbf{n}_i\}$ rotates relative to the material frame $\{\mathbf{m}_i\}$ through a rotation $\tilde{\mathbf{R}} = \mathbf{Q}^T \mathbf{R}$, i.e., $\mathbf{n}_i = \mathbf{m}_i \tilde{\mathbf{R}}$, with angle $\psi - \theta$. Clockwise rotations are considered to be positive.

associate with the material frame $\{\mathbf{m}_1, \mathbf{m}_2\}$, and repeated indices sum according to Einstein's summation convention.

In many boundary value problems used to characterize materials, the material $\{\mathbf{m}_i\}$ and natural $\{\mathbf{n}_i\}$ frames will be coincident. Pure shear is an example where all three coordinate frames are distinct [Freed and Srinivasa 2015].

To make things more precise, and to shed some light onto the subject, we cast the contravariant vector equation $d\mathbf{x} = \mathbf{F} d\mathbf{X}$ into its various component forms. First, consider a polar decomposition of the deformation gradient described by components

$$dx^i = F_j^i dX^j = R_j^i U_j^L dX^L. \quad (3a)$$

Second, consider an upper-triangular decomposition of the deformation gradient described by

$$dx^i = F_j^i dX^j = Q_\xi^i \tilde{F}_1^\xi dX^L. \quad (3b)$$

From these formulæ, it immediately follows that there also exists a displacement vector described by

$$d\tilde{x}^\xi = \tilde{F}_1^\xi dX^L = \tilde{R}_j^\xi U_j^L dX^L \quad (3c)$$

so that

$$dx^i = Q_\xi^i d\tilde{x}^\xi, \quad (3d)$$

wherein distortion $\tilde{\mathbf{F}}$ is decomposed into a polar form of $\tilde{\mathbf{F}} = \tilde{\mathbf{R}}\mathbf{U}$ with $d\tilde{\mathbf{x}} = \tilde{\mathbf{F}} d\mathbf{X}$. The deformation gradient \mathbf{F} is the same in formulæ (3a) and (3b); however, their decompositions are quite different.

We now relax our notation from that of general tensors to Cartesian tensors without loss of generality. The rotations \mathbf{R} and \mathbf{Q} in (3) are two-state fields, but the states are different between them: rotation $\mathbf{R} = R_{ij} \mathbf{e}_i \otimes \mathbf{n}_j$ vs. rotation $\mathbf{Q} = Q_{ij} \mathbf{e}_i \otimes \mathbf{m}_j$. Stretch is a Lagrangian field in that $\mathbf{U} = U_{ij} \mathbf{n}_i \otimes \mathbf{n}_j$ while distortion is a two-point tensor $\tilde{\mathbf{F}} = \tilde{F}_{ij} \mathbf{m}_i \otimes \mathbf{n}_j$ like the deformation gradient $\mathbf{F} = F_{ij} \mathbf{e}_i \otimes \mathbf{n}_j$. The matrix

representations for rotation $[\mathbf{Q}]$ and distortion $[\tilde{\mathbf{F}}]$ can be obtained in a straightforward manner from both theory and experiment, see Appendix B and Appendix C.

4. Stress power

The rate at which mechanical work is being done on a planar membrane by external tractions (forces per unit reference length), also known as the stress power, is a mechanical property that is independent of the coordinate frame used to quantify it [Hill 1978]. In the material frame $\{\mathbf{m}_i\}$, stress power becomes (see Appendix D for the derivation)

$$\dot{W} = \text{tr}(\tilde{\mathbf{S}}\tilde{\mathbf{L}}) = \tilde{S}_{11}\tilde{L}_{11} + \tilde{S}_{22}\tilde{L}_{22} + \tilde{S}_{12}\tilde{L}_{12}, \quad (4)$$

where the material stress $\tilde{\mathbf{S}} := \mathbf{Q}^T \mathbf{S} \mathbf{Q}$ has symmetric components \tilde{S}_{ij} , whereby $\tilde{\mathbf{S}} = \tilde{S}_{ij} \mathbf{m}_i \otimes \mathbf{m}_j$ with $\mathbf{S} = S_{ij} \mathbf{e}_i \otimes \mathbf{e}_j$ being the symmetric Kirchhoff [1852] stress, while the material velocity gradient $\tilde{\mathbf{L}} := \dot{\tilde{\mathbf{F}}}\tilde{\mathbf{F}}^{-1}$ has upper triangular components \tilde{L}_{ij} such that $\tilde{\mathbf{L}} = \tilde{L}_{ij} \mathbf{m}_i \otimes \mathbf{m}_j$.

Substituting the decomposition for $\tilde{\mathbf{L}}$ from (E.3) and (E.4) into formula (4) allows the stress power to be decomposed into three additive components, viz.,

$$\dot{W} = \dot{W}^\circ + \dot{W}^\square + \dot{W}^\triangleleft. \quad (5a)$$

This result is independent of any constitutive assumption to be imposed. The three constituents are:

- (1) Stress power resulting from a distortion caused by uniform dilation:

$$\dot{W}^\circ := \text{tr}(\tilde{\mathbf{S}}\tilde{\mathbf{L}}^\circ) = (\tilde{S}_{11} + \tilde{S}_{22}) \frac{1}{2}(\dot{a}/a + \dot{b}/b). \quad (5b)$$

- (2) Stress power resulting from a distortion caused by squeeze:

$$\dot{W}^\square := \text{tr}(\tilde{\mathbf{S}}\tilde{\mathbf{L}}^\square) = (\tilde{S}_{11} - \tilde{S}_{22}) \frac{1}{2}(\dot{a}/a - \dot{b}/b). \quad (5c)$$

- (3) Stress power resulting from a distortion caused by shear:

$$\dot{W}^\triangleleft := \text{tr}(\tilde{\mathbf{F}}^{-1} \tilde{\mathbf{S}} \tilde{\mathbf{F}} \tilde{\mathbf{L}}^\triangleleft) = (a/b) \tilde{S}_{12} \dot{\gamma}. \quad (5d)$$

An examination of the arguments in the traces of (5) leads one to conclude that there are two stresses to consider. One stress $\tilde{\mathbf{S}}$ for the diagonal contributions, and another stress $\tilde{\mathbf{F}}^{-1} \tilde{\mathbf{S}} \tilde{\mathbf{F}}$ for the off-diagonal contribution. This observation is consistent with Hill's findings [1978].

5. Transformed state: a basis for stress and strain

Classical constructions for describing the constitutive response of a continuum are usually formulated as an application of invariant theory [Rivlin and Smith 1969; Spencer 1972]. Criscione [2003] has argued that although the mathematical theory of invariants is elegant, its utility is flawed because of a covariance that exists between the classic invariants, thereby making parameterization of an ensuing model a daunting task. Addressing this flaw, Criscione et al. [2000; 2003a; 2003b] put forward physically based sets of strain invariants that are orthogonal to one another in the isotropic case, and nearly orthogonal to one another in the anisotropic case. Unfortunately, these strain invariants have been found to be difficult

to work with for experimentalists, and experimentalists are often the ones tasked with parameterizing some specified material model.

Motivated by Criscione's work, yet another approach for constitutive construction is put forward here. It is one possible adaptation of our hypothesis. Although we are of the opinion that there is great promise in our approach, the utility of our construction in engineering practice remains to be assessed by its users over time. Our approach is, we believe, particularly advantageous for experimentalists, see Appendix C.

The methodology put forward is not based upon invariant theory. Instead, linear transformations are introduced that establish a set of conjugate stress/strain basis pairs from which constitutive equations can be formulated in a rigorous way. In other words, we seek a set of generalized displacements q_i and their conjugate tractions p_i so that $dW = \sum_i p_i dq_i$ provides a coordinate invariant Pfaffian [Hill 1978]. Such a set is not unique, so conjugate pairs ought to be chosen where paired responses are observed to be independent of one another. As with physical laws, their presumed independence cannot be proved theoretically, only disproved experimentally, if at all. If disproved for a certain scenario, that would not necessarily invalidate the utility of a particular conjugate pairing; rather, it would bracket its range of applicability.

An inspection of (4) suggests that one introduce a set of variables expressing the stress power as

$$dW = \pi d\delta + \sigma d\varepsilon + \tau d\gamma, \quad (6)$$

where $\{\pi, \delta\}$ is a stress/strain conjugate pair of scalars describing uniform dilation, $\{\sigma, \varepsilon\}$ is a stress/strain conjugate pair of scalars describing squeeze, and $\{\tau, \gamma\}$ is a stress/strain conjugate pair of scalars describing shear. In other words, strains δ, ε and γ comprise a set of generalized displacements, viz., $\{\mathbf{q}\} = \{\delta \ \varepsilon \ \gamma\}^T$, while stresses π, σ and τ comprise a set of generalized tractions, viz., $\{\mathbf{p}\} = \{\pi \ \sigma \ \tau\}^T$, such that (6) is a coordinate-invariant description for the work of deformation dW . One admissible encoding/decoding scheme for (6) that is in accordance with our hypothesis is introduced below.

5.1. Encoding. Inspired by Becker [1893], we consider an encoding of the conjugate tensor fields $\tilde{\mathbf{S}}$ and $\tilde{\mathbf{L}}$ that describes a stress basis with constituents

$$\pi := \tilde{S}_{11} + \tilde{S}_{22}, \quad (7a)$$

$$\sigma := \tilde{S}_{11} - \tilde{S}_{22}, \quad (7b)$$

$$\tau := \frac{a}{b} \tilde{S}_{12}, \quad (7c)$$

whose conjugate strain basis (which have exact differentials for rates) has constituents

$$\delta := \ln \sqrt{ab} \quad d\delta = \frac{1}{2}(da/a + db/b), \quad (7d)$$

$$\varepsilon := \ln \sqrt{a/b} \quad \text{with} \quad d\varepsilon = \frac{1}{2}(da/a - db/b), \quad (7e)$$

$$\gamma \quad d\gamma, \quad (7f)$$

wherein parameters a, b and γ are established from \mathbf{F} via (B.2) or (B.4) for theory, and from Figure 2 and (C.1) for experiment. Each generalized displacement has a rate that is an exact differential. As such, these displacements are two-state fields, independent of the path traversed between states. Consequently, each generalized displacement defined above is a viable measure for strain. This does not, however, imply that dW is independent of path. As for the conjugate tractions, π is commonly referred to as the

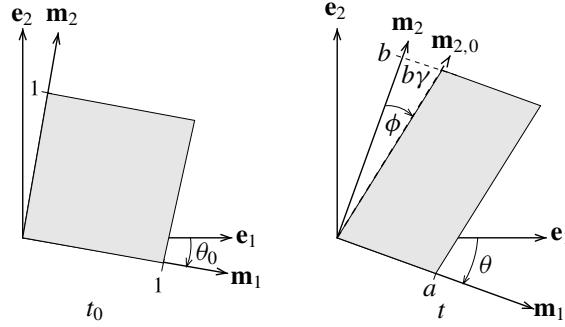


Figure 2. General kinematic analysis for the homogeneous distortion of a unit square into a parallelogram. Extensions a and b and shear $\gamma = \tan \phi$ are the kinematic parameters to be measured. Coordinate directions \mathbf{e}_1 and \mathbf{e}_2 are orthogonal, as are coordinate directions \mathbf{m}_1 and \mathbf{m}_2 . Angle θ rotates $\{\mathbf{e}_i\}$ into $\{\mathbf{m}_i\}$ and is drawn in its positive sense. Directions \mathbf{e}_1 and \mathbf{e}_2 are spatial and align with the axes of the load frame. Orthogonal axes \mathbf{m}_1 and \mathbf{m}_2 can be thought of as being painted onto the material in some reference state t_0 at a angle of θ_0 from the spatial frame $\{\mathbf{e}_i\}$. In a deformed state t , material axis \mathbf{m}_1 remains the same, now rotated by an angle of θ from the spatial frame $\{\mathbf{e}_i\}$, however, the material line originally describing the \mathbf{m}_2 direction (drawn as $\mathbf{m}_{2,0}$ in the deformed configuration) may no longer be orthogonal to \mathbf{m}_1 . The angular difference, ϕ , is the angle of shear. Direction \mathbf{m}_1 will often be selected to associate with a feature of interest in the sample being tested, e.g., a fiber direction.

surface tension, σ is the first normal stress difference found in the rheology literature [Bird et al. 1987a], and τ is a shear stress normalized by the extent of elongation that is present. Substituting (7) into (5) and rearranging leads to (6). No assumption has been made regarding material constitution. No application of invariant theory has been imposed in this construction.

Evans and Skalak [1979] and Lubarda [2010] considered a multiplicative decomposition for \mathbf{F} of $\mathbf{F} = \mathbf{F}_d \mathbf{F}_a$ wherein $\mathbf{F}_a = \sqrt{\lambda_1 \lambda_2} (\mathbf{e}_1 \otimes \mathbf{e}_1 + \mathbf{e}_2 \otimes \mathbf{e}_2)$ and $\mathbf{F}_d = (1/\sqrt{\lambda_1 \lambda_2}) (\lambda_1 \mathbf{e}_1 \otimes \mathbf{n}_1 + \lambda_2 \mathbf{e}_2 \otimes \mathbf{n}_2)$, which they call the areal and deviatoric parts of the deformation gradient, respectively, where unit vectors \mathbf{n}_1 and \mathbf{n}_2 are the eigenvectors of stretch (they are not the Lagrangian base vectors). Our decomposition is similar in purpose to theirs, but distinct in form and physics from theirs.

5.2. Decoding. For an encoding to be admissible, there must be a unique decoding such that the overall encoding/decoding algorithm is one-to-one. The decoding that associates with the encoding put forward in (7) describes a distortion tensor $\tilde{\mathbf{F}}$ that populates as

$$[\tilde{\mathbf{F}}] = \begin{bmatrix} e^\delta & 0 \\ 0 & e^\delta \end{bmatrix} \begin{bmatrix} e^\epsilon & 0 \\ 0 & e^{-\epsilon} \end{bmatrix} \begin{bmatrix} 1 & \gamma \\ 0 & 1 \end{bmatrix} = \begin{bmatrix} e^{\delta+\epsilon} & e^{\delta+\epsilon} \gamma \\ 0 & e^{\delta-\epsilon} \end{bmatrix}, \quad (8a)$$

with an inverse of

$$[\tilde{\mathbf{F}}]^{-1} = \begin{bmatrix} 1 & -\gamma \\ 0 & 1 \end{bmatrix} \begin{bmatrix} e^{-\epsilon} & 0 \\ 0 & e^\epsilon \end{bmatrix} \begin{bmatrix} e^{-\delta} & 0 \\ 0 & e^{-\delta} \end{bmatrix} = \begin{bmatrix} e^{-\epsilon-\delta} & -e^{\epsilon-\delta} \gamma \\ 0 & e^{\epsilon-\delta} \end{bmatrix}, \quad (8b)$$

whose affiliated material velocity gradient $\tilde{\mathbf{L}}$ populates as

$$[\tilde{\mathbf{L}}] = \begin{bmatrix} \dot{\delta} & 0 \\ 0 & \dot{\delta} \end{bmatrix} + \begin{bmatrix} \dot{\varepsilon} & 0 \\ 0 & -\dot{\varepsilon} \end{bmatrix} + \begin{bmatrix} 0 & e^{2\varepsilon} \dot{\gamma} \\ 0 & 0 \end{bmatrix} = \begin{bmatrix} \dot{\delta} + \dot{\varepsilon} & e^{2\varepsilon} \dot{\gamma} \\ 0 & \dot{\delta} - \dot{\varepsilon} \end{bmatrix}. \quad (8c)$$

Because the deformation \mathbf{F} and velocity $\mathbf{L} := \dot{\mathbf{F}}\mathbf{F}^{-1}$ gradients are typically known *a priori*, the material rotation \mathbf{Q} and spin $\mathbf{\Xi} := \dot{\mathbf{Q}}\mathbf{Q}^T$ tensors follow immediately via

$$\mathbf{Q} = \mathbf{F}\tilde{\mathbf{F}}^{-1} \quad \text{and} \quad \mathbf{\Xi} = \mathbf{W} - \tilde{\mathbf{W}}, \quad (8d)$$

with $\mathbf{W} := \frac{1}{2}(\mathbf{L} - \mathbf{L}^T)$ and $\tilde{\mathbf{W}} := \frac{1}{2}(\tilde{\mathbf{L}} - \tilde{\mathbf{L}}^T)$ being their respective vorticities.

Furthermore, the material stress tensor populates according to a decoding scheme of

$$[\tilde{\mathbf{S}}] = \frac{1}{2} \begin{bmatrix} \pi & 0 \\ 0 & \pi \end{bmatrix} + \frac{1}{2} \begin{bmatrix} \sigma & 0 \\ 0 & -\sigma \end{bmatrix} + \begin{bmatrix} 0 & e^{-2\varepsilon} \tau \\ e^{-2\varepsilon} \tau & 0 \end{bmatrix} = \begin{bmatrix} \frac{1}{2}(\pi + \sigma) & e^{-2\varepsilon} \tau \\ e^{-2\varepsilon} \tau & \frac{1}{2}(\pi - \sigma) \end{bmatrix}, \quad (9a)$$

where stresses π , σ and τ are usually quantified through constitutive equations, but could also be measured experimentally, see Appendix C. The material stress rate therefore populates as

$$\dot{[\tilde{\mathbf{S}}]} = \begin{bmatrix} \frac{1}{2}(\dot{\pi} + \dot{\sigma}) & e^{-2\varepsilon}(\dot{\tau} - 2\tau\dot{\varepsilon}) \\ e^{-2\varepsilon}(\dot{\tau} - 2\tau\dot{\varepsilon}) & \frac{1}{2}(\dot{\pi} - \dot{\sigma}) \end{bmatrix}, \quad (9b)$$

that when rotated into the Eulerian frame becomes

$$\dot{\mathbf{S}} = \mathbf{Q}\dot{\tilde{\mathbf{S}}}\mathbf{Q}^T, \quad \dot{\mathbf{S}} := \frac{d\mathbf{S}}{dt} + \mathbf{S}\mathbf{\Xi} - \mathbf{\Xi}\mathbf{S} \quad \text{where} \quad \mathbf{S} = \mathbf{Q}\tilde{\mathbf{S}}\mathbf{Q}^T, \quad (9c)$$

with \mathbf{S} being the symmetric Kirchhoff [1852] stress, $d\mathbf{S}/dt$ being its material derivative, and $\dot{\mathbf{S}}$ describing an objective corotational rate. This objective rate is akin to the polar rate of Green and Naghdi [1965] and Dienes [1979], but with \mathbf{Q} replacing \mathbf{R} .

A brief discussion of rate is in order. The question to be answered is this: in what frame does the *material*, not the observer, sense its environment? It is in that frame that the appropriate time derivative to use is the partial derivative. We stipulate that it is within an embedded coordinate frame where this occurs, as developed by Oldroyd [1950] and adopted by his followers, e.g., [Bird et al. 1987a; 1987b; Lodge 1964; 1974]. These constructions employ general tensor fields defined over curvilinear coordinate frames whose coordinate axes are described by the same set of material particles over time. Within the confines of Cartesian tensors, the material frame $\{\mathbf{m}_i\}$ is the closest that one can get to mimicking an embedded curvilinear coordinate frame, because the \mathbf{m}_1 coordinate line remains tangent to the 1 material curve, and the 12 coordinate plane with normal $\mathbf{m}_1 \times \mathbf{m}_2$ remains tangent to the 12 material surface [Freed and Srinivasa 2015; Srinivasa 2012]. They are tangents at the origin of coordinate frame $\{\mathbf{m}_1, \mathbf{m}_2, \mathbf{m}_3\}$. It is here where the partial derivative most accurately approximates its actual physical rate, within the confines of employing rectangular Cartesian tensors.

5.3. Encoding/decoding maps. To show the one-to-one mapping property of this encoding/decoding algorithm, the generalized displacement rates obey the linear mapping

$$\begin{Bmatrix} \dot{q}_1 \\ \dot{q}_2 \\ \dot{q}_3 \end{Bmatrix} := \begin{Bmatrix} \dot{\delta} \\ \dot{\varepsilon} \\ \dot{\gamma} \end{Bmatrix} = \begin{bmatrix} 1/2 & 1/2 & 0 \\ 1/2 & -1/2 & 0 \\ 0 & 0 & e^{-2\varepsilon} \end{bmatrix} \begin{Bmatrix} \tilde{L}_{11} \\ \tilde{L}_{22} \\ \tilde{L}_{12} \end{Bmatrix}, \quad (10a)$$

while their associated tractions obey the linear mapping

$$\begin{Bmatrix} p_1 \\ p_2 \\ p_3 \end{Bmatrix} := \begin{Bmatrix} \pi \\ \sigma \\ \tau \end{Bmatrix} = \begin{bmatrix} 1 & 1 & 0 \\ 1 & -1 & 0 \\ 0 & 0 & e^{2\varepsilon} \end{bmatrix} \begin{Bmatrix} \tilde{S}_{11} \\ \tilde{S}_{22} \\ \tilde{S}_{12} \end{Bmatrix}, \quad (10b)$$

which are invertible maps in that

$$\begin{Bmatrix} \tilde{L}_{11} \\ \tilde{L}_{22} \\ \tilde{L}_{12} \end{Bmatrix} = \begin{bmatrix} 1 & 1 & 0 \\ 1 & -1 & 0 \\ 0 & 0 & e^{2\varepsilon} \end{bmatrix} \begin{Bmatrix} \dot{\delta} \\ \dot{\varepsilon} \\ \dot{\gamma} \end{Bmatrix} \quad (11a)$$

and

$$\begin{Bmatrix} \tilde{S}_{11} \\ \tilde{S}_{22} \\ \tilde{S}_{12} \end{Bmatrix} = \begin{bmatrix} 1/2 & 1/2 & 0 \\ 1/2 & -1/2 & 0 \\ 0 & 0 & e^{-2\varepsilon} \end{bmatrix} \begin{Bmatrix} \pi \\ \sigma \\ \tau \end{Bmatrix}, \quad (11b)$$

where $\tilde{S}_{21} = \tilde{S}_{12}$. These are maps between continuum mechanics variables and generalized thermodynamic variables. They obey $\dot{W} = \tilde{S}_{11}\tilde{L}_{11} + \tilde{S}_{22}\tilde{L}_{22} + \tilde{S}_{12}\tilde{L}_{12} = \pi\dot{\delta} + \sigma\dot{\varepsilon} + \tau\dot{\gamma}$, as they must. Selecting an encoding/decoding map is key to one's construction of a model that satisfies our hypothesis. It is akin to selecting a set of invariants to use for constitutive construction, but no invariants have been used here.

The encoding/decoding algorithm of (7)–(11) describes an isotropic material response in the sense that an imposed state of uniform stress (i.e., $\pi > 0$, $\sigma = 0$ and $\tau = 0$) will cause a uniform response in strain (viz., $\delta > 0$, $\varepsilon = 0$ and $\gamma = 0$). An encoding/decoding algorithm better suited for describing anisotropic materials, both 2D and 3D, has been developed and will be introduced in a separate paper.

An isotropic membrane whose response is taken to be a function of the symmetric stretch tensor will have two independent modes of deformation: dilation and shear. However, an isotropic membrane whose response is taken to be a function of the triangular distortion tensor will have three independent modes of deformation: dilation, squeeze and shear. This is consistent with Murnaghan's [1954] theoretical finding that a symmetric 2×2 matrix has two invariants, while a triangular 2×2 matrix has three invariants, see Appendix A.1 and Appendix B.2.

6. Constitutive relations

An elastic solid can conduct heat, but does not convert work into heat over a closed cycle. This defines an elastic body [Rajagopal 2011]. The second law of thermodynamics, when describing a reversible process, as interpreted by Carathéodory [1909], implicates that an integrating factor (temperature $T > 0$) exists that transforms the first law of thermodynamics, an *inexact differential equation*, into an *exact differential equation* that becomes $dS = 1/T(dU - 1/\rho_0 dW)$ for a solid continuum [Kestin and Rice 1970]. This is

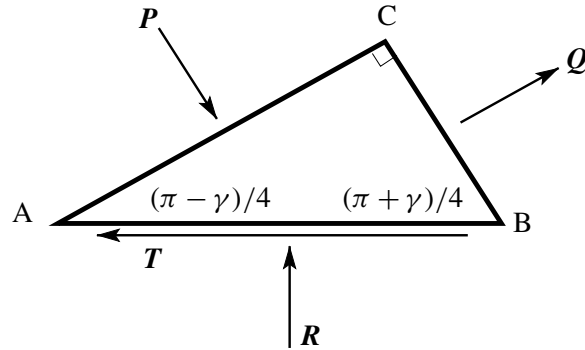


Figure 3. Poynting's [1909] stress analysis of simple shear. Forces \mathbf{P} and \mathbf{Q} align with the principal axes of stretch, therefore, there are no shears acting on these faces. Their axes are rotated $\gamma/4$ radians from the $\pm 45^\circ$ diagonals, where γ is the extent of shear. Forces \mathbf{R} and \mathbf{T} are the normal and shear forces acting on the plane of shear. Triangle ABC is a right triangle whose sides have lengths $AB = 2\ell$ and $AC = \sqrt{2}\ell(1 + \frac{1}{4}\gamma + \frac{3}{32}\gamma^2)$ and $BC = \sqrt{2}\ell(1 - \frac{1}{4}\gamma + \frac{3}{32}\gamma^2)$. His analysis is accurate to second order.

the second law of thermodynamics governing a reversible process wherein U denotes the internal energy and S denotes the entropy, both per unit mass. Introducing the Legendre transformation $A = U - TS$ allows one to rewrite the second law as $dT = -1/S(dA - 1/\rho_0 dW)$, where A is the Helmholtz free energy per unit mass, with entropy S now being the integrating factor. Theories for elasticity follow forthwith.

6.1. Thermodynamic couplings. Two couplings that exist between conjugate pairs in a thermodynamic state are the Kelvin [Thomson 1878] and Poynting [1909] effects. The Kelvin effect is a first-order effect where a change in temperature causes a change in volume. The Poynting effect is a second-order effect where a shear causes a lengthening normal to the shear plane that, if constrained in the sense of a simple shear experiment, will lead to a compressive normal stress. The former effect is well known; the latter effect is less so. They are handled as constitutive characteristics in our approach.

The Kelvin effect is typically modeled in three space as $\Delta V = 3\alpha\Delta T$ where a change in volume ΔV is proportional to a change in temperature ΔT with α being the constant of proportionality, i.e., the coefficient of thermal strain.

Figure 3 presents an overview of Poynting's stress analysis for simple shear. In a change of notation, he considered a second-order response with principle tractions of $\|\mathbf{P}\|/AC = G_1\gamma - (\frac{1}{2}G_1 - G_2)\gamma^2$ and $\|\mathbf{Q}\|/BC = G_1\gamma + (\frac{1}{2}G_1 - G_2)\gamma^2$. Applying this notation to Poynting's analysis, he determined that the components of traction acting upon the plane of shear are $\|\mathbf{T}\|/AB = G_1\gamma$ and $\|\mathbf{R}\|/AB = -G_2\gamma^2$ wherein G_1 is the linear shear modulus of Lamé while G_2 is a second-order shear modulus introduced by Poynting. In the material frame $\{\mathbf{m}_i\}$, traction $\|\mathbf{T}\|/AB$ equates with \tilde{S}_{12} and traction $\|\mathbf{R}\|/AB$ equates with $-\tilde{S}_{22}$, while the stress component \tilde{S}_{11} is zero.

6.2. Explicit elasticity. A Green [1848] elastic solid assumes that the Helmholtz free energy is a state function whose variation is described by an exact differential in state, namely, temperature and strain

[Ogden 1984]. In terms of the decomposition of work put forward in (6), the second law takes on a form of

$$\rho_0 \left(\frac{\partial A}{\partial T} dT + \frac{\partial A}{\partial \delta} d\delta + \frac{\partial A}{\partial \varepsilon} d\varepsilon + \frac{\partial A}{\partial \gamma} d\gamma \right) = -\rho_0 S dT + \pi d\delta + \sigma d\varepsilon + \tau d\gamma, \quad (12)$$

which — because the temperature T , strain from dilation δ , strain from squeeze ε , and strain from shear γ can all be varied separately and independently of one another (at least in principle) — requires that the coefficients to differentials dT , $d\delta$, $d\varepsilon$ and $d\gamma$ must each vanish individually, leading to the following set of constitutive formulæ:

$$S = -\frac{\partial A}{\partial T}, \quad \pi = \rho_0 \frac{\partial A}{\partial \delta}, \quad \sigma = \rho_0 \frac{\partial A}{\partial \varepsilon}, \quad \tau = \rho_0 \frac{\partial A}{\partial \gamma}. \quad (13)$$

These constitutive equations govern a planar Green elastic solid within the context of our theoretical approach. Alternatively, Srinivasa [2012] derived a Green elastic solid in terms of the six upper-triangular components of the distortion tensor $\tilde{\mathbf{F}}$ in three-space.

6.2.1. A Hooke–Kelvin–Poynting solid. Consider a planar solid whose Helmholtz free-energy function takes on the form of

$$\rho_0 A = -C(T \ln(T/T_0) - (T - T_0)) + 2K(\delta - \alpha(T - T_0))^2 + M\varepsilon^2 + \left(\frac{1}{2}G_1 + G_2(\varepsilon - \delta)\right)\gamma^2, \quad (14)$$

where C is the heat capacity and α is Kelvin’s coefficient of thermal strain, both of which reference to some temperature T_0 , while K , M and G_1 are akin to the bulk modulus, the P-wave modulus, and the shear modulus from linear elasticity, as they apply to 2-space, with G_2 being Poynting’s second-order shear modulus.

Substituting this energy function into our elastic theory (13) produces the set of constitutive formulæ:

$$\rho_0 S = C \ln(T/T_0) + 4\alpha K(\delta - \alpha(T - T_0)), \quad (15a)$$

$$\pi = 4K(\delta - \alpha(T - T_0)) - G_2\gamma^2, \quad (15b)$$

$$\sigma = 2M\varepsilon + G_2\gamma^2, \quad (15c)$$

$$\tau = (G_1 + 2G_2(\varepsilon - \delta))\gamma, \quad (15d)$$

which describe an elastic planar solid in the material frame $\{\mathbf{m}_i\}$ where the deformation gradient is decomposed into an orthogonal rotation matrix and an upper-triangular distortion matrix (see Appendix B). This model accounts for both the Kelvin [Thomson 1878] and Poynting [1909] effects.

Poisson’s Ratio: In linear elasticity, the ratio of transverse strain to axial strain caused by an axial traction, when multiplied by minus one to make it positive valued, is a material constant known as Poisson’s ratio ν . In nonlinear elasticity, this ratio is a response function, not a material constant. In our analysis, $\ln a$ is the axial strain while $\ln b$ is the transverse strain in a simple extension, see Appendix B. Because stresses π and σ in (9) are equal during such a loading, (15) describes a Poisson’s response of

$$\nu := -\frac{\ln b}{\ln a} \Bigg|_{\substack{\tilde{s}_{22}=0 \\ \tilde{s}_{12}=0}} \equiv -\frac{\delta - \varepsilon}{\delta + \varepsilon} \Bigg|_{\substack{\pi=\sigma \\ \tau=0}} = \frac{2K - M}{2K + M}, \quad (16)$$

so that, e.g., the ratio $\nu = \frac{1}{2}$ whenever $K = \frac{3}{2}M$, the ratio $\nu = \frac{1}{3}$ whenever $K = M$, and the ratio $\nu = 0$ whenever $K = \frac{1}{2}M$. Consequently, both K and M can be parameterized from a single uniaxial experiment, leaving G_1 and G_2 to be parameterized from a shear experiment.

6.2.2. Solution strategy. This scheme assumes that one is given a temperature T and a deformation gradient \mathbf{F} and seeks its associated entropy density S and Kirchhoff stress \mathbf{S} .

Begin by computing extensions a and b and shear γ from (B.4) and then calculate the trigonometric functions $\cos \theta$ and $\sin \theta$ from (B.5) from which rotation \mathbf{Q} can be established via (B.3a). Now determine the conjugate strains $\{\delta, \varepsilon, \gamma\}$ using the encoding algorithm of (7d)–(7f). Solve the constitutive equations (15) for the entropy S and conjugate stresses $\{\pi, \sigma, \tau\}$. Using these generalized stresses and the imposed squeeze strain ε , populate the material stress $\tilde{\mathbf{S}}$ using the decoding algorithm of (9a), which rotates into the Eulerian Kirchhoff stress \mathbf{S} via \mathbf{Q} according to (9c).

6.3. Implicit elasticity. An implicit elastic solid assumes that the energy function A depends upon temperature, strain *and* stress [Rajagopal 2003]. It cannot, however, depend upon both temperature and entropy, as it depends upon both strain and stress, because either the temperature T or the entropy S is the integrating factor for the second law, depending upon the thermodynamic potential selected. In terms of the decomposition of work put forward in (6), the second law of thermodynamics takes on a form of

$$\rho_0 \left(\frac{\partial A}{\partial T} dT + \frac{\partial A}{\partial \delta} d\delta + \frac{\partial A}{\partial \pi} d\pi + \frac{\partial A}{\partial \varepsilon} d\varepsilon + \frac{\partial A}{\partial \sigma} d\sigma + \frac{\partial A}{\partial \gamma} d\gamma + \frac{\partial A}{\partial \tau} d\tau \right) = -\rho_0 S dT + \pi d\delta + \sigma d\varepsilon + \tau d\gamma \quad (17)$$

which — because the temperature T , the dilation response $\{\delta, \pi\}$, the squeeze response $\{\varepsilon, \sigma\}$, and the shear response $\{\gamma, \tau\}$ can all be varied separately and independently of one another (at least in principle) — allows one to separate causalities resulting in the following set of constitutive formulae:

$$S = -\frac{\partial A}{\partial T}, \quad (18a)$$

$$\pi d\delta = \rho_0 \frac{\partial A}{\partial \delta} d\delta + \rho_0 \frac{\partial A}{\partial \pi} d\pi, \quad (18b)$$

$$\sigma d\varepsilon = \rho_0 \frac{\partial A}{\partial \varepsilon} d\varepsilon + \rho_0 \frac{\partial A}{\partial \sigma} d\sigma, \quad (18c)$$

$$\tau d\gamma = \rho_0 \frac{\partial A}{\partial \gamma} d\gamma + \rho_0 \frac{\partial A}{\partial \tau} d\tau, \quad (18d)$$

where the governing equations for the stress/strain response are now described by an implicit system of ordinary differential equations.

As our interest from this point on resides with modeling soft biological tissues, we forgo addressing the coupling effects of Kelvin [Thomson 1878] and Poynting [1909]. We can safely neglect the Kelvin effect because mammals regulate their temperature. We neglect the Poynting effect as a simplification. How this second-order geometric effect is to be accounted for in a material that itself is highly nonlinear is a subject for future study. Furthermore, there is no experimental data known to us by which one could substantiate such a theory.

6.3.1. Strain-limiting solid. Extrapolating the energy function put forward by Freed and Rajagopal [2016] for an isothermal implicit strain-limiting elastic fiber into an energy function that is suitable for a planar

elastic membrane implicates

$$\rho_0 A = 4K\delta - \pi + \beta^\circ \pi \delta + 2M\varepsilon - \sigma + \beta^\square \sigma \varepsilon + G\gamma - \tau + \beta^\angle \tau \gamma, \quad (19)$$

where K , M and G are moduli describing tangent responses at zero stress and zero strain with β° , β^\square and β^\angle relating to their respective states of limiting strain: $\beta^\circ = 1/\delta_{\max}$, $\beta^\square = 1/\varepsilon_{\max}$ and $\beta^\angle = 1/\gamma_{\max}$. Substituting the energy function in (19) into the constitutive theory of (18) produces an implicit strain-limiting planar elastic solid described by the following system of differential equations:

$$\frac{d\pi}{d\delta} = \frac{4K + (\beta^\circ - 1)\pi}{1 - \beta^\circ \delta}, \quad (20a)$$

$$\frac{d\sigma}{d\varepsilon} = \frac{2M + (\beta^\square - 1)\sigma}{1 - \beta^\square \varepsilon}, \quad (20b)$$

$$\frac{d\tau}{d\gamma} = \frac{G + (\beta^\angle - 1)\tau}{1 - \beta^\angle \gamma}, \quad (20c)$$

whose solution, by the separation of variables, describes a dilatonic response of

$$\pi = \frac{4K}{\beta^\circ - 1} \left(\frac{1}{(1 - \beta^\circ \langle \delta \rangle)^{(\beta^\circ - 1)/\beta^\circ}} - 1 \right) \quad \beta^\circ > 1, \quad (21a)$$

a squeeze response of

$$\sigma = \operatorname{sgn}(\varepsilon) \frac{2M}{\beta^\square - 1} \left(\frac{1}{(1 - \beta^\square |\varepsilon|)^{(\beta^\square - 1)/\beta^\square}} - 1 \right) \quad \beta^\square > 1, \quad (21b)$$

and a shear response of

$$\tau = \operatorname{sgn}(\gamma) \frac{G}{\beta^\angle - 1} \left(\frac{1}{(1 - \beta^\angle |\gamma|)^{(\beta^\angle - 1)/\beta^\angle}} - 1 \right) \quad \beta^\angle > 1. \quad (21c)$$

These formulæ are written so strain causes stress. They can be written where stress causes strain [Freed and Rajagopal 2016].

Formulæ (21b) and (21c) have been adjusted so that the stresses they produce are odd functions of their respective strains. Both positive and negative squeeze and shear stresses can be supported by membranes, provided that any negative contribution arising from squeeze is offset by a positive dilation. In contrast, only positive dilations can be supported by a membrane. Negative dilations would wrinkle a membrane, which is why the Macaulay bracket $\langle \delta \rangle$ is introduced into formula (21a) with values for $\langle \delta \rangle$ being δ whenever $\delta \geq 0$ and 0 otherwise. This aspect of the model could be made more robust through an application of tension-field theory [Pipkin 1986; Steigmann 1990], but that lies beyond the scope of the present paper.

6.3.2. Solution strategy. This scheme assumes that one is given a deformation gradient \mathbf{F} and seeks its associated Kirchhoff stress \mathbf{S} . It is possible that a submitted \mathbf{F} can be invalid, so a strategy needs to be constructed to handle inadmissible deformation gradients. A more robust scheme would return strains for supplied stresses, but that strategy does not align as well with finite element formulations.

Begin by computing extensions a and b and shear γ from (B.4) and then calculate the trigonometric functions $\cos \theta$ and $\sin \theta$ from (B.5) from which rotation \mathbf{Q} can be established via (B.3a). Now determine

the conjugate strains $\{\delta, \varepsilon, \gamma\}$ using the encoding algorithm in (7d)–(7f). Test to ensure $0 \leq \delta < 1/\beta^\circ$ and $|\varepsilon| < 1/\beta^\square$ and $|\gamma| < 1/\beta^\angle$. If none of these constraints are violated then continue, otherwise the supplied deformation gradient \mathbf{F} is inadmissible and must be handled. Solve the constitutive equations (21) for the conjugate stresses $\{\pi, \sigma, \tau\}$. Using these generalized stresses and the imposed squeeze strain ε , populate the material stress $\tilde{\mathbf{S}}$ using the decoding algorithm in (9a), which rotates into the Eulerian Kirchhoff stress \mathbf{S} via \mathbf{Q} according to (9c).

6.4. A model for biological membranes. Freed and Rajagopal [2016] modeled collagen fibers as a non-linear implicit elastic solid intertwined with a linear Hookean solid such that their compliances add, with the outcome being a material response that is characteristic of most soft biologic materials. Here a stress/strain curve starts out with a compliant nonlinear response and finishes up with a stiff linear response. Their fiber model has three material constants whose values are unique, physical and visible within a stress/strain curve, as shown in Figure 4. Their conjecture, applied here to each stress/strain basis pair in \mathbb{R}^2 , leads to the following set of three constitutive equations: one for the dilatoric response,

$$\delta = \frac{\langle \pi \rangle}{4K^C} + \frac{1}{\beta^\circ} \left(1 - \frac{1}{(1 + (\beta^\circ - 1)\langle \pi \rangle / 4K^E)^{\beta^\circ / (\beta^\circ - 1)}} \right) \quad \beta^\circ > 1, \quad (22a)$$

one for the squeeze response,

$$\varepsilon = \frac{\sigma}{2M^C} + \frac{\text{sgn}(\sigma)}{\beta^\square} \left(1 - \frac{1}{(1 + (\beta^\square - 1)|\sigma| / 2M^E)^{\beta^\square / (\beta^\square - 1)}} \right) \quad \beta^\square > 1, \quad (22b)$$

and one for the shear response,

$$\gamma = \frac{\tau}{G^C} + \frac{\text{sgn}(\tau)}{\beta^\angle} \left(1 - \frac{1}{(1 + (\beta^\angle - 1)|\tau| / G^E)^{\beta^\angle / (\beta^\angle - 1)}} \right) \quad \beta^\angle > 1, \quad (22c)$$

which are expressed so that stresses cause strains. Moduli K^C ($> K^E > 0$) and M^C ($> M^E > 0$) and G^C ($> G^E > 0$) are the terminating elastic moduli that describe deformation in their respective linear regions, whereat collagen is the predominant load bearing constituent. Moduli K^E , M^E and G^E are the elastic moduli caused by the restoring forces of elastin that crimp the collagen fibrils in a neighborhood surrounding zero stress and zero strain; while β° ($= 1/\delta_{\max}^E$) and β^\square ($= 1/\varepsilon_{\max}^E$) and β^\angle ($= 1/\gamma_{\max}^E$) are reciprocal measures for the three limiting states of configuration strain whereat, for soft tissues, the crimp of collagen has been stretched taut. These are illustrated in Figure 4.

6.4.1. Solution strategy. This scheme assumes that one is given a deformation gradient \mathbf{F} along with an initial guess for the Kirchhoff stress \mathbf{S} whose actual value is being sought.

Begin by computing extensions a and b and shear γ from (B.4) and then calculate the trigonometric functions $\cos \theta$ and $\sin \theta$ from (B.5) from which rotation \mathbf{Q} can be established via (B.3a). Now determine the assigned conjugate strains $\{\delta, \varepsilon, \gamma\}$ using the encoding algorithm of (7d)–(7f). Rotate the guessed value for Kirchhoff stress \mathbf{S} into the material frame using \mathbf{Q} to get $\tilde{\mathbf{S}}$ according to (9c). Encode the conjugate stresses $\{\pi, \sigma, \tau\}$ using (7a)–(7c) and use these to solve the constitutive equations (22) to get predicted values for the conjugate strains $\{\delta, \varepsilon, \gamma\}$. Use a root finding algorithm to secure a set of conjugate stresses whose associated conjugate strains are in error with the assigned conjugate strains by less than some specified tolerance. Using the converged values for these conjugate stresses and the

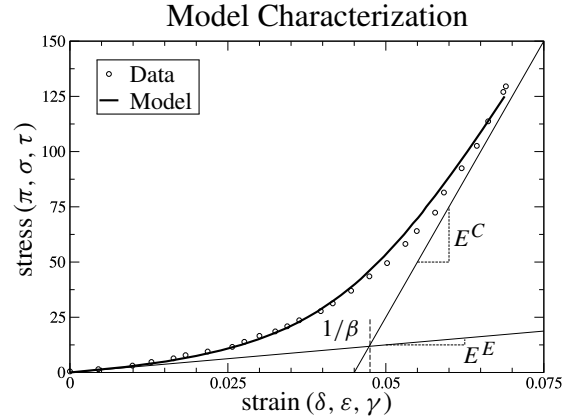


Figure 4. Representative plot depicting the tensile response for the three modes of model (22). Modulus $E^E \in \{K^E, M^E, G^E\}$ describes the low-stress asymptotic behavior where elastin governs the constitutive response, while modulus $E^C \in \{K^C, M^C, G^C\}$ describes the high-stress asymptotic behavior where collagen governs the constitutive response. The intersection of these two asymptotic lines is the reciprocal to parameter $\beta \in \{\beta^\circ, \beta^\square, \beta^\triangleleft\}$ with $1/\beta$ designating the strain where collagen crimp stretches straight.

imposed squeeze strain ε , populate the material stress $\tilde{\mathbf{S}}$ using the decoding algorithm in (9a), which rotates into the Eulerian Kirchhoff stress \mathbf{S} via \mathbf{Q} according to (9c).

7. Experiments

A procedure is outlined in Appendix C for extracting the conjugate stresses π, σ, τ and strains $\delta, \varepsilon, \gamma$ from a planar experiment, along with the angular rotation θ between the material and Eulerian frames.

At present, there is no single experimental data set that we are aware of that would allow one to quantify all three modes of planar deformation introduced in this paper. Consequently, a parameterization of our model (22) using data extracted from a single experiment possessing sensitivity to all model parameters is not currently possible, nor is it for Fung's [1993, p. 304] planar model, in that regard. Both are constitutive equations in nine parameters under isothermal conditions. Plans have been put into motion to address this deficiency from which the data set will be rich enough to provide sensitivity sufficient for quantifying all model parameters. As for now, we are content with demonstrating that our material model (22) is reasonable and worthy of further consideration and scrutiny.

Ideally, one would perform three separate experiments: one for each mode or conjugate pair. One where $\{\pi, \delta\}$ vary and the other fields are held fixed, one where $\{\sigma, \varepsilon\}$ vary and the other fields are held fixed, and one where $\{\tau, \gamma\}$ vary and the other fields are held fixed. Here we analyze published data for dilation and shear, but there is no published data where squeeze is the sole mechanism of deformation. Fortunately, there is data where dilation exists both by itself and in conjunction with squeeze so that the response of both modes can be extracted and studied.

Figure 5 presents data acquired from a double-lap shear test done on porcine myocardium by Dokos et al. [2002, Figure 4], tabulated in [Freed 2014, Table 7.3]. They represent a passive shear response

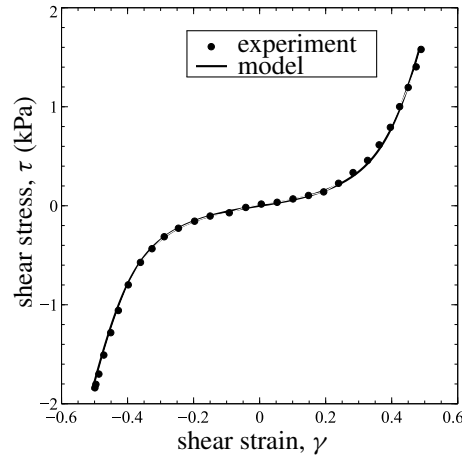


Figure 5. Loading behavior of a porcine myocardium under simple shear. The points represent experimental data. The curve represents the response of model (22c) with $G^C = 15$ kPa, $G^E = 0.5$ kPa and $\beta^L = 2.5$.

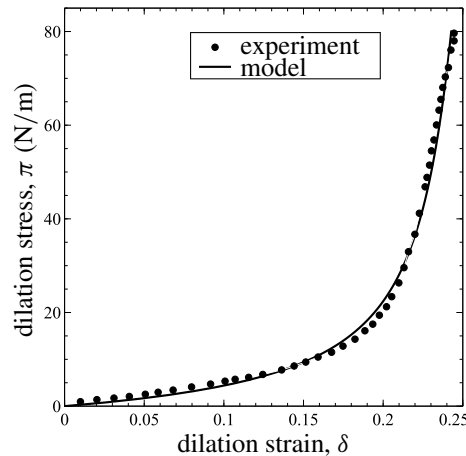


Figure 6. Dilation behavior of a porcine visceral pleural membrane under equibiaxial loading conditions. The points represent experimental data. The curve represents the response of model (22a) with $K^C = 1,875$ N/m, $K^E = 7$ N/m and $\beta^\circ = 4.1$.

for muscle. Only the loading portion of the curve is shown. Viscoelastic effects will be addressed in a future paper. Our shear model (22c) does an excellent job of describing the nonlinear behavior exhibited by these data.

Figure 6 presents data from an equibiaxial test done on porcine visceral pleura by Freed, Liao and Einstein [2014]. Our dilation model (22a) does a nice job of describing the nonlinear behavior displayed by these data, too.

A planar biaxial loading sequence was imposed on a visceral pleural membrane in the study cited above. Specifically, an equibiaxial 1:1 loading was followed in sequence by two proportional loadings with orthogonal traction ratios of 2:1 and 1:2. Figure 7 presents the squeeze response from these three

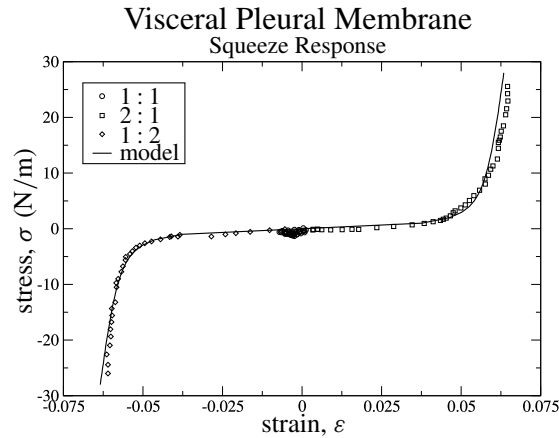


Figure 7. Squeeze behavior of a porcine visceral pleural membrane under three proportional loading conditions. The points represent experimental data. The curve represents the response of model (22b) with $M^C = 2500$ N/m, $M^E = 5$ N/m and $\beta^D = 17$.

experiments. The response from the 2:1 traction ratio produced the data in the first quadrant, while the response from the 1:2 traction ratio produced the data in the third quadrant. The equibiaxial experiment produces noise around the origin in the squeeze domain, as it ought; dilation and squeeze are independent deformation modes according to our theory. Our squeeze model (22b) provides a nice description for these data as well.

There is a very large difference in the strain limits for dilation and squeeze in the visceral pleural membrane, viz., $1/\beta^D = 0.24$ and $1/\beta^S = 0.06$, respectively. This lends further credence to our conjecture that these two modes of deformation are independent of one another.

Equation (16) is applicable for establishing Poisson's ratio in a neighborhood around zero stress, in which case we found $\nu = 0.47$ because $K^E = 7$ N/m and $M^E = 5$ N/m. This is consistent with values reported throughout the literature on Poisson's ratio for soft biological tissues.

To further substantiate our methodology, the dilations from these three proportional experiments are shown in Figure 8 along with the model correlation from Figure 6. The response from the 2:1 protocol is in reasonable agreement with the equibiaxial experiment. The 1:2 protocol was the last leg executed in the loading sequence imposed on this sample. Several slip-stick events caused by tissue tearing at suture incision points occurred during the 1:2 loading leg [Freed, Liao and Einstein 2014] and are a likely cause for why their dilation data in Figure 8 are offset from those of the other two protocols. Tearing also had an effect on the squeeze response recorded in Figure 7 causing a small translation of the strain response toward the origin in the third quadrant, but it is less noticeable there.

8. Summary

An elastic theory for planar biological membranes has been derived from thermodynamics and applied to data reported in the literature. The theory is unique in that it is based upon conjugate stress/strain basis pairs, not invariants. These pairs are generalized thermodynamic variables. Constitutive equations were derived for explicit and implicit elastic solids that, when combined, produce a model suitable for soft

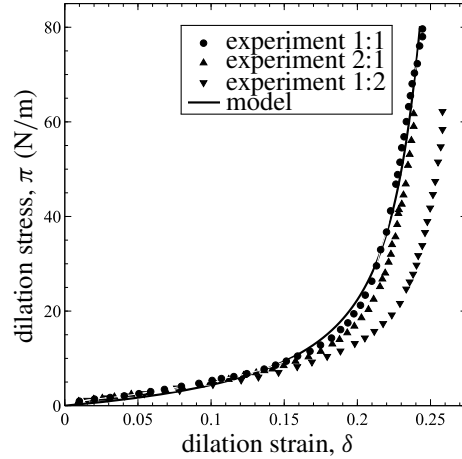


Figure 8. Dilation behavior of a porcine visceral pleural membrane under three proportional loading conditions. The points represent experimental data. The curve represents the model response taken from Figure 6.

tissues. The resulting constitutive formulæ produce a power-law response through the toe and heel regions that culminate with a linear terminal response, indicative of the behavior exhibited by most soft biological tissues whose extracellular matrix consists of collagen fibers intertwined with an elastin network. Data from biaxial experiments done on myocardium and visceral pleura substantiate the model.

Appendix A: Polar decomposition of \mathbf{F}

Because $\det \mathbf{F} > 0$ from the conservation of mass, the deformation gradient \mathbf{F} will have a unique matrix decomposition of $[\mathbf{F}] = [\mathbf{R}][\mathbf{U}]$ where matrix $[\mathbf{R}]$ has orthonormal columns and matrix $[\mathbf{U}]$ is symmetric with positive eigenvalues [Noll 1955].

Quantifying a polar decomposition of the deformation gradient, i.e., $\mathbf{F} = \mathbf{R}\mathbf{U}$, see [Simo and Hughes 1998], begins with computing the eigenvalues for stretch via

$$\lambda_1 = \sqrt{\frac{1}{2}((C_{11} + C_{22}) + \sqrt{(C_{11} + C_{22})^2 - 4(C_{11}C_{22} - C_{12}^2)})}, \quad (\text{A.1a})$$

$$\lambda_2 = \sqrt{\frac{1}{2}((C_{11} + C_{22}) - \sqrt{(C_{11} + C_{22})^2 - 4(C_{11}C_{22} - C_{12}^2)})}, \quad (\text{A.1b})$$

where the symmetric Cauchy deformation tensor $\mathbf{C} = \mathbf{F}^T \mathbf{F}$ has components $\mathbf{C} = C_{ij} \mathbf{n}_i \otimes \mathbf{n}_j$ evaluated in the Lagrangian frame $\{\mathbf{n}_1, \mathbf{n}_2\}$. Knowing the principal stretches, one can populate the matrices for the Lagrangian stretch $[\mathbf{U}]$ and its inverse $[\mathbf{U}]^{-1}$ via the formulæ [Ting 1985]:

$$[\mathbf{U}] = \frac{1}{I} (II[\mathbf{I}] + [\mathbf{C}]), \quad (\text{A.2a})$$

$$[\mathbf{U}]^{-1} = \frac{1}{I II} ((I^2 - II)[\mathbf{I}] - [\mathbf{C}]), \quad (\text{A.2b})$$

where the two invariants I and II of stretch are described by

$$I = \lambda_1 + \lambda_2 \quad \text{and} \quad II = \lambda_1 \lambda_2. \quad (\text{A.3})$$

The rotation matrix $[\mathbf{R}]$ determined from $[\mathbf{R}] = [\mathbf{F}][\mathbf{U}]^{-1}$ becomes

$$[\mathbf{R}] = \begin{bmatrix} \cos \psi & \sin \psi \\ -\sin \psi & \cos \psi \end{bmatrix}, \quad (\text{A.4a})$$

wherein, from (A.1)–(A.3),

$$\psi = \begin{cases} \sin^{-1}([(I^2 - II - C_{22})F_{12} - C_{12}F_{11}]/(I II)), \\ \sin^{-1}([(C_{11} - I^2 + II)F_{21} + C_{12}F_{22}]/(I II)), \end{cases} \quad (\text{A.4b})$$

where ψ is a rotation angle that orients the natural frame $\{\mathbf{n}_i\}$ relative to the Eulerian frame $\{\mathbf{e}_i\}$, as drawn in Figure 1, and is positive for clockwise rotations and negative for counterclockwise rotations.

A.1. Invariants. A symmetric 2×2 matrix, say $[\mathbf{A}]$, with elements

$$[\mathbf{A}] = \begin{bmatrix} a & c \\ c & b \end{bmatrix} \quad (\text{A.5a})$$

in some coordinate frame $\{\mathbf{e}_1, \mathbf{e}_2\}$, rotates via some orthogonal matrix $[\mathbf{R}]$ into another coordinate frame $\{\hat{\mathbf{e}}_1, \hat{\mathbf{e}}_2\}$ where $\hat{\mathbf{e}}_i = \mathbf{e}_i \mathbf{R}$ with the matrix mapping as $[\hat{\mathbf{A}}] = [\mathbf{R}]^T [\mathbf{A}] [\mathbf{R}]$. A function of matrix $[\mathbf{A}]$, say $f(\mathbf{A})$, is invariant under arbitrary rotations provided that

$$f(\mathbf{A}) = f(\hat{\mathbf{A}}) = f(\mathbf{R}^T \mathbf{A} \mathbf{R}). \quad (\text{A.5b})$$

It is well known that the trace and determinant obey this condition, resulting in the two invariants

$$I_1 = a + b \quad \text{and} \quad I_2 = ab - c^2, \quad (\text{A.5c})$$

wherein $I_1 := \text{tr}(\mathbf{R}^T \mathbf{A} \mathbf{R}) = \text{tr}(\mathbf{R} \mathbf{R}^T \mathbf{A}) = \text{tr}(\mathbf{A})$ and $I_2 := \det(\mathbf{R}^T \mathbf{A} \mathbf{R}) = \det(\mathbf{R}^T) \det(\mathbf{A}) \det(\mathbf{R}) = \det(\mathbf{A})$ and therefore $\text{tr}(\mathbf{A}^2) = I_1^2 - 2I_2$. In the case of stretch, (A.3) and (A.5c) are equivalent, with (A.3) being described in principal (spectral) coordinates.

Appendix B: QR decomposition of \mathbf{F}

Because $\det \mathbf{F} > 0$ from the conservation of mass, the deformation gradient \mathbf{F} will have another unique matrix decomposition of $[\mathbf{F}] = [\mathbf{Q}][\tilde{\mathbf{F}}]$ where matrix $[\mathbf{Q}]$ has orthonormal columns (distinct from $[\mathbf{R}]$) and matrix $[\tilde{\mathbf{F}}]$ is upper triangular with positive diagonal elements [Stewart 1973].

Quantifying a QR decomposition of the deformation gradient, i.e., $[\mathbf{F}] = [\mathbf{Q}][\tilde{\mathbf{F}}]$, leads to a distortion $[\tilde{\mathbf{F}}]$ and its inverse $[\tilde{\mathbf{F}}]^{-1}$ that populate via [Freed and Srinivasa 2015]

$$[\tilde{\mathbf{F}}] = \begin{bmatrix} a & a\gamma \\ 0 & b \end{bmatrix} \quad \text{and} \quad [\tilde{\mathbf{F}}]^{-1} = \begin{bmatrix} 1/a & -\gamma/b \\ 0 & 1/b \end{bmatrix}, \quad (\text{B.1})$$

whose constituents are established through a Cholesky factorization of $\mathbf{C} = \mathbf{F}^T \mathbf{F} = \tilde{\mathbf{F}}^T \tilde{\mathbf{F}}$ leading to [Srinivasa 2012]

$$a = \sqrt{C_{11}}, \quad \gamma = C_{12}/C_{11}, \quad b = \sqrt{C_{22} - C_{12}^2/C_{11}}, \quad (\text{B.2})$$

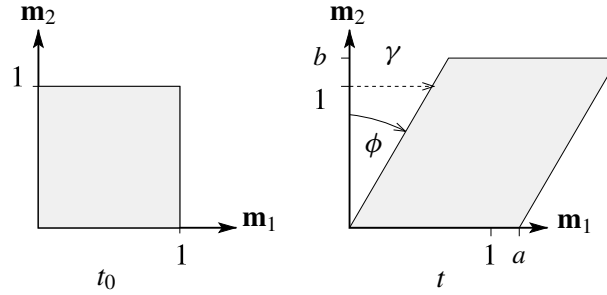


Figure 9. The homogeneous distortion of a unit square into a parallelogram. Extensions a and b and shear $\gamma = \tan \phi$ are the kinematic parameters to be measured in a planar experiment to quantify distortion $\tilde{\mathbf{F}}$ via (B.1) in the $\{\mathbf{m}_i\}$ coordinate frame.

where parameters a , b and γ are physical quantities that can be extracted from experiment (see Appendix C). Measurements are to be made in accordance with Figure 9. Parameter a is the extension ratio in the \mathbf{m}_1 direction, viz., $a = \ell_1(t)/\ell_1(t_0)$. Parameter b is the extension ratio in the \mathbf{m}_2 direction, viz., $b = \ell_2(t)/\ell_2(t_0)$. Parameter γ measures the extent that a material line originally aligned with the \mathbf{m}_2 direction rotates in the \mathbf{m}_1 direction — an extent described by $\gamma = \tan \phi$, wherein ϕ is the shear angle. Extensions a and b and stretches λ_1 and λ_2 are coincident only in the absence of shear γ , otherwise they are distinct quantities. Rosakis [1990, Lemma 5.1] has proven that $\lambda_1 \geq a \geq \lambda_2$, where λ_1 and λ_2 are the eigenvalues of stretch given in (A.1).

The rotational contribution $[\mathbf{Q}]$ arising from an upper-triangular decomposition of the deformation gradient is determined from $[\mathbf{Q}] = [\mathbf{F}][\tilde{\mathbf{F}}]^{-1}$ and (B.1) and (B.2) leading to

$$[\mathbf{Q}] = \begin{bmatrix} \cos \theta & \sin \theta \\ -\sin \theta & \cos \theta \end{bmatrix}, \quad (\text{B.3a})$$

wherein

$$\theta = \begin{cases} -\sin^{-1}(F_{21}/a), \\ \sin^{-1}((F_{12} - \gamma F_{11})/b), \end{cases} \quad (\text{B.3b})$$

with θ being the angle that the material frame $\{\mathbf{m}_i\}$ rotates relative to the Eulerian frame $\{\mathbf{e}_i\}$ with positive rotations occurring in a clockwise sense, see, Figure 1.

Recall that the angle of rotation of the Lagrangian frame $\{\mathbf{n}_i\}$ relative to the Eulerian frame $\{\mathbf{e}_i\}$ is ψ , see (A.4). Consequently, angle $\psi - \theta$ establishes the angle of rotation of the Lagrangian frame $\{\mathbf{n}_i\}$ about the material frame $\{\mathbf{m}_i\}$, see, Figure 1.

B.1. Derived from the deformation gradient. Alternatively, one can use the components of the deformation gradient $[\mathbf{F}]$ to directly quantify extensions a and b and shear γ , the building blocks of distortion $[\tilde{\mathbf{F}}]$, plus the angle θ that determines rotation $[\mathbf{Q}]$ between the Eulerian $\{\mathbf{e}_i\}$ and material $\{\mathbf{m}_i\}$ coordinate frames via

$$a = \sqrt{F_{11}^2 + F_{21}^2}, \quad \gamma = \frac{F_{11}F_{12} + F_{21}F_{22}}{F_{11}^2 + F_{21}^2}, \quad b = \frac{F_{11}F_{22} - F_{12}F_{21}}{\sqrt{F_{11}^2 + F_{21}^2}}, \quad (\text{B.4})$$

with

$$\sin \theta = \frac{-F_{21}}{\sqrt{F_{11}^2 + F_{21}^2}} \quad \text{and} \quad \cos \theta = \frac{F_{11}}{\sqrt{F_{11}^2 + F_{21}^2}}, \quad (\text{B.5})$$

thereby foregoing any need to construct the Cauchy deformation tensor \mathbf{C} .

B.2. Invariants. An upper-triangular 2×2 matrix, say $[\mathbf{A}]$, with elements

$$[\mathbf{A}] = \begin{bmatrix} a & c \\ 0 & b \end{bmatrix} \quad (\text{B.6})$$

has three unitary invariants [Murnaghan 1954]:

$$\bar{I}_1 = \text{tr}(\mathbf{A}) = a + b, \quad \bar{I}_2 = \text{tr}(\mathbf{A}^2) = a^2 + b^2, \quad \bar{I}_3 = \text{tr}(\mathbf{A}^\top \mathbf{A}) = a^2 + b^2 + c^2, \quad (\text{B.7})$$

where \bar{I}_1 , \bar{I}_2 and \bar{I}_3 are invariant of coordinate rotations because $\text{tr}(\mathbf{R}^\top \mathbf{A} \mathbf{R}) = \text{tr}(\mathbf{R} \mathbf{R}^\top \mathbf{A}) = \text{tr}(\mathbf{A}) = \bar{I}_1$ and $\text{tr}((\mathbf{R}^\top \mathbf{A} \mathbf{R})(\mathbf{R}^\top \mathbf{A} \mathbf{R})) = \text{tr}(\mathbf{R}^\top \mathbf{A} \mathbf{A} \mathbf{R}) = \text{tr}(\mathbf{R} \mathbf{R}^\top \mathbf{A}^2) = \text{tr}(\mathbf{A}^2) = \bar{I}_2$, and because $\text{tr}((\mathbf{R}^\top \mathbf{A} \mathbf{R})^\top (\mathbf{R}^\top \mathbf{A} \mathbf{R})) = \text{tr}(\mathbf{R}^\top \mathbf{A}^\top \mathbf{R} \mathbf{R}^\top \mathbf{A} \mathbf{R}) = \text{tr}(\mathbf{R}^\top \mathbf{A}^\top \mathbf{A} \mathbf{R}) = \text{tr}(\mathbf{R} \mathbf{R}^\top \mathbf{A}^\top \mathbf{A}) = \text{tr}(\mathbf{A}^\top \mathbf{A}) = \bar{I}_3$. It follows that $\det \mathbf{A} = \frac{1}{2}(\bar{I}_1^2 - \bar{I}_2)$. The extra invariant follows because matrix $[\mathbf{A}]$ is upper triangular and therefore $[\mathbf{A}]^2$ is upper triangular whereas $[\mathbf{A}]^\top [\mathbf{A}]$ is symmetric.

Appendix C: Experimentation

Lanir and Fung [1974], Humphrey et al. [1987], Sacks [1999; 2000] and others have been perfecting the planar biaxial-stretch experiment for over four decades, as it applies to testing soft biological tissues. Our analysis of this experiment assumes homogeneous deformation and incorporates an upper triangular decomposition of the deformation gradient to quantify deformation and stress from experimental observations.

C.1. Deformation. An experimental assessment of deformation is straightforward. Extensions a and b and shear $\gamma = \tan \phi$ are the kinematic parameters to be acquired. Their values are directly observed and readily measured in accordance with Figure 2. Once they are known, the distortion matrix $[\tilde{\mathbf{F}}]$ can be populated according to (B.1). Coordinate directions \mathbf{e}_1 and \mathbf{e}_2 are orthogonal, as are coordinate directions \mathbf{m}_1 and \mathbf{m}_2 . Angle θ rotates $\{\mathbf{e}_i\}$ into $\{\mathbf{m}_i\}$ and is drawn in its positive sense in Figure 2. With θ measured and known, one can populate the rotation matrix $[\mathbf{Q}]$ according to (B.3a).

Axes \mathbf{m}_1 and \mathbf{m}_2 can be thought of as being painted onto the material in some reference state t_0 oriented at an angle of θ_0 with respect to the spatial frame $\{\mathbf{e}_i\}$ so that initially

$$[\mathbf{F}_0] = \begin{bmatrix} \cos \theta_0 & \sin \theta_0 \\ -\sin \theta_0 & \cos \theta_0 \end{bmatrix}. \quad (\text{C.1a})$$

In a deformed state t , material axis \mathbf{m}_1 remains a material axis, now rotated by an angle of θ from the spatial frame $\{\mathbf{e}_i\}$, however, the material line originally drawn in the \mathbf{m}_2 direction (drawn as $\mathbf{m}_{2,0}$ in Figure 2) may no longer be orthogonal to \mathbf{m}_1 at times $t > t_0$. Any angular difference (from being a right angle) is caused by shear and quantified by $\phi = \tan^{-1} \gamma$. The deformation gradient is now given by

$$[\mathbf{F}] = [\mathbf{Q}][\tilde{\mathbf{F}}] = \begin{bmatrix} \cos \theta & \sin \theta \\ -\sin \theta & \cos \theta \end{bmatrix} \begin{bmatrix} a & a\gamma \\ 0 & b \end{bmatrix} = \begin{bmatrix} a \cos \theta & b \sin \theta + a\gamma \cos \theta \\ -a \sin \theta & b \cos \theta - a\gamma \sin \theta \end{bmatrix}. \quad (\text{C.1b})$$

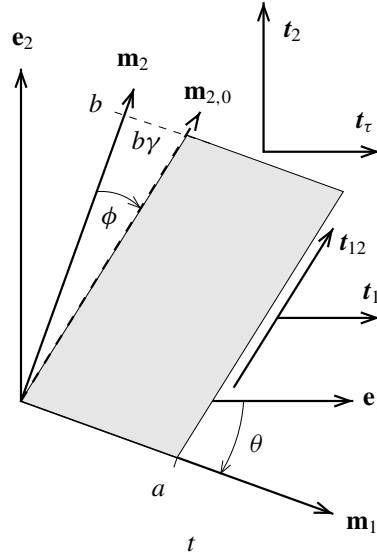


Figure 10. In-plane loading of a sample that was originally square and has undergone biaxial extension through orthogonal tractions f_1 and f_2 applied in the \mathbf{e}_1 and \mathbf{e}_2 directions, respectively, and have also undergone a shear through a traction f_τ applied in the \mathbf{e}_1 direction, e.g., in the geometric sense of a double-lap shear. These three tractions have units of force per unit undeformed length of line, as measured in a reference state at time t_0 where $a = b = 1$ and $\gamma = 0$. In a deformed state, say at current time t , the actual tractions are $t_1 = f_1/b\sqrt{1 + \gamma^2}$ and $t_2 = f_2/a$ and $t_\tau = f_\tau/a$ and have units of force per unit deformed length of line, where $\gamma = \tan \phi$. Traction t_{12} is an internal reaction caused by the grips. It cannot be controlled by the experimentalist. It exists to conserve angular momentum.

Direction \mathbf{m}_1 will often be selected to associate with a feature of interest in the sample being tested, e.g., aligned with a fiber direction.

This kinematic assessment is valid for any homogeneous planar deformation. It is general.

C.2. Stress. Stresses are more challenging to get, but the process is fairly straightforward. Cauchy's [1827] fundamental theorem for stress implies that $\mathbf{t} = \mathbf{T}\mathbf{n}$ where $\mathbf{t} = t_i\mathbf{e}_i$ is a traction vector, $\mathbf{T} = T_{ij}\mathbf{e}_i \otimes \mathbf{e}_j$ is Cauchy's stress tensor, and $\mathbf{n} = n_i\mathbf{e}_i$ is a unit normal to the surface upon which traction \mathbf{t} acts. All fields are defined in the Eulerian frame $\{\mathbf{e}_1, \mathbf{e}_2\}$. The symmetric Kirchhoff [1852] stress, also an Eulerian field, is defined by $\mathbf{S} := \det(\mathbf{F})\mathbf{T} = S_{ij}\mathbf{e}_i \otimes \mathbf{e}_j$, where $\det \mathbf{F} = ab$ for membranes. Cauchy's theorem for stress rotates into the material frame $\{\mathbf{m}_i\}$ to become $\tilde{\mathbf{t}} = 1/(ab)\tilde{\mathbf{S}}\tilde{\mathbf{n}}$ wherein $\tilde{\mathbf{t}} = \mathbf{Q}^T\mathbf{t}$ and $\tilde{\mathbf{n}} = \mathbf{Q}^T\mathbf{n}$ and $\tilde{\mathbf{S}} = \mathbf{Q}^T\mathbf{S}\mathbf{Q}$. It is formula $\tilde{\mathbf{t}} = 1/(ab)\tilde{\mathbf{S}}\tilde{\mathbf{n}}$ that we choose to apply to quantify stress in the material frame $\{\mathbf{m}_1, \mathbf{m}_2\}$.

When it comes to stress, each experiment is a separate boundary value problem. There is no general result like there is for deformation. Here we consider the experiment illustrated in Figure 10. Data extracted from such an experiment would be rich enough to ensure sensitivity for all parameters in our material model (22), hence our interest in this experiment.

To aid in avoiding wrinkling over a range of interest in shear strain, a sample would ideally be exposed to positive tractions in the 1 and 2 directions, denoted as t_1 and t_2 in Figure 10. After the membrane

is supporting surface tension, to offset the onset of wrinkling, one would impose a traction of shear t_τ through, e.g., a double-lap shear gripping configuration (traction t_{12} present in Figure 10 is not under the control of an experimentalist. It is an internal traction caused by the grips).

In accordance with Figure 10, an application of Cauchy's theorem to the two edges of the areal element in that figure, solving for stress components in the $\{\mathbf{m}_i\}$ coordinate frame, leads to

$$\begin{Bmatrix} t_1 \cos \theta + t_{12} \sin \phi \\ t_1 \sin \theta + t_{12} \cos \phi \end{Bmatrix} = \frac{1}{ab} \begin{bmatrix} \tilde{S}_{11} & \tilde{S}_{12} \\ \tilde{S}_{21} & \tilde{S}_{22} \end{bmatrix} \begin{Bmatrix} \cos \phi \\ -\sin \phi \end{Bmatrix} \quad (\text{C.2a})$$

and

$$\begin{Bmatrix} -t_2 \sin \theta + t_\tau \cos \theta \\ t_2 \cos \theta + t_\tau \sin \theta \end{Bmatrix} = \frac{1}{ab} \begin{bmatrix} \tilde{S}_{11} & \tilde{S}_{12} \\ \tilde{S}_{21} & \tilde{S}_{22} \end{bmatrix} \begin{Bmatrix} 0 \\ 1 \end{Bmatrix} \quad (\text{C.2b})$$

that comprise a linear system of equations which, when solved for the components of stress \tilde{S}_{ij} , yields

$$\tilde{S}_{11} = a(\cos \theta f_1 + b\gamma t_{12}) + b\gamma(\cos \theta f_\tau - \sin \theta f_2), \quad (\text{C.3a})$$

$$\tilde{S}_{12} = \tilde{S}_{21} = b(\cos \theta f_\tau - \sin \theta f_2), \quad (\text{C.3b})$$

$$\tilde{S}_{22} = b(\sin \theta f_\tau + \cos \theta f_2), \quad (\text{C.3c})$$

where, from symmetry of $\tilde{\mathbf{S}}$, i.e., $\tilde{S}_{21} = \tilde{S}_{12}$, one determines that

$$t_{12} = \frac{-a \sin \theta \cos \phi f_1 - b \sin(\theta + \phi) f_2 + b \cos(\theta + \phi) f_\tau}{ab \cos \phi}, \quad (\text{C.3d})$$

wherein tractions f_1 , f_2 and f_τ have units of force per unit undeformed length of line. They associate with tractions t_1 , t_2 and t_τ , which have units of force per unit deformed length of line, via the formulæ

$$f_1 = b \sec \phi t_1, \quad f_2 = at_2, \quad f_\tau = at_\tau. \quad (\text{C.4})$$

From (7a)–(7c), one finds that the conjugate stresses have values of

$$\pi = a(\cos \theta f_1 + b\gamma t_{12}) + b((\sin \theta + \gamma \cos \theta) f_\tau + (\cos \theta - \gamma \sin \theta) f_2), \quad (\text{C.5a})$$

$$\sigma = a(\cos \theta f_1 + b\gamma t_{12}) - b((\sin \theta - \gamma \cos \theta) f_\tau + (\cos \theta + \gamma \sin \theta) f_2), \quad (\text{C.5b})$$

$$\tau = a(\cos \theta f_\tau - \sin \theta f_2), \quad (\text{C.5c})$$

and therefore an experimentalist needs to measure the three tractions f_1 , f_2 and f_τ and the three deformations a , b and γ in order to quantify the three conjugate states of stress π , σ and τ .

These formulæ will simplify under a variety of special conditions, e.g., whenever $\theta = \phi = 0$ and $f_\tau = 0$, (C.5) simplifies to

$$\pi = af_1 + bf_2, \quad \sigma = af_1 - bf_2, \quad \tau = 0, \quad (\text{C.6})$$

which describe the boundary condition used in the experiments of Lanir and Fung [1974], Humphrey et al. [1987], Sacks [1999; 2000], Billiar and Sacks [2000b; 2000a], Freed, Liao and Einstein [2014] and numerous others.

Appendix D: Derivation of Equation (4)

We begin with the well known description for stress power [Ogden 1984]:

$$\dot{W} = \text{tr}(\mathbf{P}^\top \dot{\mathbf{F}}), \quad (\text{D.1})$$

and then apply properties of the trace. This allows one to rewrite the above expression as

$$\dot{W} = \text{tr}(\mathbf{P}^\top \dot{\mathbf{F}}) = \text{tr}(\mathbf{F}\mathbf{P}^\top \dot{\mathbf{F}}\mathbf{F}^{-1}) = \text{tr}(\mathbf{S}\dot{\mathbf{L}}), \quad (\text{D.2})$$

because stress \mathbf{S} is symmetric and therefore $\mathbf{S} = \mathbf{P}\mathbf{F}^\top = \mathbf{F}\mathbf{P}^\top$. Incorporating the triangular decomposition of the deformation gradient established in Appendix B permits one to rewrite the above equation as

$$\dot{W} = \text{tr}(\mathbf{S}\dot{\mathbf{L}}) = \text{tr}(\mathbf{S}\dot{\mathbf{F}}\mathbf{F}^{-1}) = \text{tr}(\mathbf{S}\dot{\mathbf{Q}}\tilde{\mathbf{F}}\tilde{\mathbf{F}}^{-1}\mathbf{Q}^{-1}) + \text{tr}(\mathbf{S}\dot{\mathbf{Q}}\tilde{\mathbf{F}}\tilde{\mathbf{F}}^{-1}\mathbf{Q}^{-1}). \quad (\text{D.3})$$

The first trace on the right-hand side is zero because the Kirchhoff stress $\mathbf{S} = S_{ij}\mathbf{e}_i \otimes \mathbf{e}_j$ is symmetric while spin $\boldsymbol{\Xi} = \mathbf{Q}\mathbf{Q}^\top = \Xi_{ij}\mathbf{e}_i \otimes \mathbf{e}_j$ is skew symmetric, therefore $\text{tr}(\mathbf{S}\dot{\mathbf{Q}}\tilde{\mathbf{F}}\tilde{\mathbf{F}}^{-1}\mathbf{Q}^{-1}) = \text{tr}(\mathbf{S}\dot{\mathbf{Q}}\mathbf{Q}^\top) = \text{tr}(\mathbf{S}\boldsymbol{\Xi}) = 0$. Rearranging the second trace leads to

$$\dot{W} = \text{tr}(\mathbf{Q}^\top \mathbf{S}\dot{\mathbf{Q}}\tilde{\mathbf{F}}\tilde{\mathbf{F}}^{-1}) = \text{tr}(\tilde{\mathbf{S}}\dot{\tilde{\mathbf{L}}}), \quad (\text{D.4})$$

wherein $\tilde{\mathbf{S}} := \mathbf{Q}^\top \mathbf{S}\mathbf{Q} = \tilde{S}_{ij}\mathbf{m}_i \otimes \mathbf{m}_j$ and $\tilde{\mathbf{L}} := \dot{\tilde{\mathbf{F}}}\tilde{\mathbf{F}}^{-1} = \tilde{L}_{ij}\mathbf{m}_i \otimes \mathbf{m}_j$, as established in (E.4). Because $\tilde{\mathbf{S}}$ is symmetric and $\tilde{\mathbf{L}}$ is upper triangular,

$$\text{tr}\left(\begin{bmatrix} \tilde{S}_{11} & \tilde{S}_{12} \\ \tilde{S}_{12} & \tilde{S}_{22} \end{bmatrix} \begin{bmatrix} \tilde{L}_{11} & \tilde{L}_{12} \\ 0 & \tilde{L}_{22} \end{bmatrix}\right) = \tilde{S}_{11}\tilde{L}_{11} + \tilde{S}_{12}\tilde{L}_{12} + \tilde{S}_{22}\tilde{L}_{22}, \quad (\text{D.5})$$

which proves (4).

Appendix E: Decomposition of distortion $\tilde{\mathbf{F}}$

The distortion tensor $\tilde{\mathbf{F}}$ in (B.1) can be decomposed into a product of three fundamental modes of deformation, e.g., $\tilde{\mathbf{F}} = \tilde{\mathbf{F}}^\circ \tilde{\mathbf{F}}^\square \tilde{\mathbf{F}}^\angle$ with matrix components

$$[\tilde{\mathbf{F}}^\circ][\tilde{\mathbf{F}}^\square][\tilde{\mathbf{F}}^\angle] = \underbrace{\begin{bmatrix} \sqrt{ab} & 0 \\ 0 & \sqrt{ab} \end{bmatrix}}_{\text{dilation}} \underbrace{\begin{bmatrix} \sqrt{a/b} & 0 \\ 0 & \sqrt{b/a} \end{bmatrix}}_{\text{squeeze}} \underbrace{\begin{bmatrix} 1 & \gamma \\ 0 & 1 \end{bmatrix}}_{\text{shear}} = \begin{bmatrix} a & a\gamma \\ 0 & b \end{bmatrix} = [\tilde{\mathbf{F}}], \quad (\text{E.1})$$

where dilation $\tilde{\mathbf{F}}^\circ$ is a uniform contribution to distortion, squeeze $\tilde{\mathbf{F}}^\square$ is an extrusion-like contribution to distortion², and shear $\tilde{\mathbf{F}}^\angle$ is an angular contribution to distortion. The distortions of dilation and squeeze commute, because they are diagonal, and as such $\tilde{\mathbf{F}}^\circ \tilde{\mathbf{F}}^\square = \tilde{\mathbf{F}}^\square \tilde{\mathbf{F}}^\circ$. The distortions of squeeze and shear are isometric, because they preserve area, and as such $\det \tilde{\mathbf{F}}^\square = \det \tilde{\mathbf{F}}^\angle = 1$.

² Freed and Srinivasa [2015] refer to $\tilde{\mathbf{F}}^\square$ as extrusion. Here we call it squeeze to give it a more intuitive terminology to a wider audience. It describes an isometric deformation that maps a square \square into a rectangle \square of the same area. It is similar to (but distinct from) pure shear [Freed and Srinivasa 2015].

E.1. Rates of distortion. Differentiating the decomposition of distortion (E.1) by the product rule gives

$$\begin{aligned}
\dot{\tilde{\mathbf{F}}} &= \dot{\tilde{\mathbf{F}}^\circ} \tilde{\mathbf{F}} \tilde{\mathbf{F}}^\angle + \tilde{\mathbf{F}}^\circ \dot{\tilde{\mathbf{F}}^\square} \tilde{\mathbf{F}}^\angle + \tilde{\mathbf{F}}^\circ \tilde{\mathbf{F}}^\square \dot{\tilde{\mathbf{F}}^\angle} \\
&= \dot{\tilde{\mathbf{F}}^\circ} \tilde{\mathbf{F}} \tilde{\mathbf{F}}^\angle + \dot{\tilde{\mathbf{F}}^\square} \tilde{\mathbf{F}}^\circ \tilde{\mathbf{F}}^\angle + \tilde{\mathbf{F}}^\circ \tilde{\mathbf{F}}^\square \dot{\tilde{\mathbf{F}}^\angle} \\
&= \dot{\tilde{\mathbf{F}}^\circ} (\tilde{\mathbf{F}}^\circ)^{-1} \tilde{\mathbf{F}} + \dot{\tilde{\mathbf{F}}^\square} (\tilde{\mathbf{F}}^\square)^{-1} \tilde{\mathbf{F}} + \tilde{\mathbf{F}} (\tilde{\mathbf{F}}^\angle)^{-1} \dot{\tilde{\mathbf{F}}^\angle} \\
&= \tilde{\mathbf{L}}^\circ \tilde{\mathbf{F}} + \tilde{\mathbf{L}}^\square \tilde{\mathbf{F}} + \tilde{\mathbf{F}} \tilde{\mathbf{L}}^\angle,
\end{aligned} \tag{E.2}$$

where, to advance from the first line to the second, we use the fact that $\tilde{\mathbf{F}}^\circ$ and $\tilde{\mathbf{F}}^\square$ commute. Identities, e.g., $\mathbf{I} = (\tilde{\mathbf{F}}^\circ)^{-1} \tilde{\mathbf{F}}^\circ$, along with (E.1) advance the second line to the third. Going from the third line to the fourth is done by defining velocity gradients for the three modes comprising the rate of distortion:

(1) For dilation, define $\tilde{\mathbf{L}}^\circ := \dot{\tilde{\mathbf{F}}^\circ} (\tilde{\mathbf{F}}^\circ)^{-1} = (\tilde{\mathbf{F}}^\circ)^{-1} \dot{\tilde{\mathbf{F}}^\circ}$ whose matrix components are

$$[\tilde{\mathbf{L}}^\circ] = \frac{1}{2} \left(\frac{\dot{a}}{a} + \frac{\dot{b}}{b} \right) \begin{bmatrix} 1 & 0 \\ 0 & 1 \end{bmatrix}. \tag{E.3a}$$

(2) For squeeze, define $\tilde{\mathbf{L}}^\square := \dot{\tilde{\mathbf{F}}^\square} (\tilde{\mathbf{F}}^\square)^{-1} = (\tilde{\mathbf{F}}^\square)^{-1} \dot{\tilde{\mathbf{F}}^\square}$ whose matrix components are

$$[\tilde{\mathbf{L}}^\square] = \frac{1}{2} \left(\frac{\dot{a}}{a} - \frac{\dot{b}}{b} \right) \begin{bmatrix} 1 & 0 \\ 0 & -1 \end{bmatrix}. \tag{E.3b}$$

(3) For shear, define $\tilde{\mathbf{L}}^\angle := \dot{\tilde{\mathbf{F}}^\angle} (\tilde{\mathbf{F}}^\angle)^{-1} = (\tilde{\mathbf{F}}^\angle)^{-1} \dot{\tilde{\mathbf{F}}^\angle}$ whose matrix components are

$$[\tilde{\mathbf{L}}^\angle] = \begin{bmatrix} 0 & \dot{\gamma} \\ 0 & 0 \end{bmatrix}. \tag{E.3c}$$

It turns out that the material velocity gradients $\tilde{\mathbf{L}}^\circ$, $\tilde{\mathbf{L}}^\square$ and $\tilde{\mathbf{L}}^\angle$ commute in the products that define them.

The three material velocity gradients that are defined in (E.3) sum according to (E.2) to form a log-like rate of distortion that is defined by $\tilde{\mathbf{L}} := \dot{\tilde{\mathbf{F}}} \tilde{\mathbf{F}}^{-1} = \tilde{\mathbf{L}}^\circ + \tilde{\mathbf{L}}^\square + \tilde{\mathbf{F}} \tilde{\mathbf{L}}^\angle \tilde{\mathbf{F}}^{-1}$ with matrix components³

$$[\tilde{\mathbf{L}}] = \begin{bmatrix} \dot{a}/a & a\dot{\gamma}/b \\ 0 & \dot{b}/b \end{bmatrix}. \tag{E.4}$$

The Eulerian velocity gradient $\mathbf{L} := \dot{\mathbf{F}} \mathbf{F}^{-1}$ and the material velocity gradient $\tilde{\mathbf{L}} := \dot{\tilde{\mathbf{F}}} \tilde{\mathbf{F}}^{-1}$ relate to one another through the expression

$$\begin{aligned}
\tilde{\mathbf{L}} &= \mathbf{Q}^\top (\mathbf{L} - \boldsymbol{\Xi}) \mathbf{Q}, \\
&= \mathbf{Q}^\top \mathbf{L} \mathbf{Q} - \boldsymbol{\Xi},
\end{aligned} \quad \text{wherein} \quad [\boldsymbol{\Xi}] = \begin{bmatrix} 0 & \dot{\theta} \\ -\dot{\theta} & 0 \end{bmatrix} \tag{E.5}$$

with spin $\boldsymbol{\Xi} := \dot{\mathbf{Q}} \mathbf{Q}^\top$, an Eulerian field, designating the rate at which the material frame $\{\mathbf{m}_i\}$ rotates about the Eulerian frame $\{\mathbf{e}_i\}$ with θ being defined in (B.3b) and drawn in Figure 1. The skew symmetric part of (E.5) produces the useful result

$$\boldsymbol{\Xi} = \mathbf{W} - \tilde{\mathbf{W}}, \tag{30}$$

³ Freed and Srinivasa [2015] define $\tilde{\mathbf{L}}$ as $\tilde{\mathbf{F}}^{-1} \dot{\tilde{\mathbf{F}}}$, whereas we define it as $\dot{\tilde{\mathbf{F}}} \tilde{\mathbf{F}}^{-1}$. They derived the logarithm of distortion $\ln \tilde{\mathbf{F}}$ whose rate is not $\tilde{\mathbf{L}}$. The diagonal components of $\tilde{\mathbf{L}}$ and $\ln \tilde{\mathbf{F}}$ are the same; it is in the off-diagonal components that they differ.

stated in (8d), where $\mathbf{W} := \frac{1}{2}(\mathbf{L} - \mathbf{L}^T)$ and $\tilde{\mathbf{W}} := \frac{1}{2}(\tilde{\mathbf{L}} - \tilde{\mathbf{L}}^T)$ are the spatial and material vorticities.

Remark. An important but subtle point is that $\tilde{\mathbf{L}}$ is not integrable, because $\tilde{\mathbf{F}}\tilde{\mathbf{L}}\tilde{\mathbf{F}}^{-1}$ is not integrable, and therefore $\tilde{\mathbf{L}}$ is not a viable measure for strain rate. Strain is a field that depends only upon its two end states, and not upon the path traversed to get from one state to the other. Consequently, *strain rate must be described by an exact differential*, and $\tilde{\mathbf{L}}$ is not an exact differential.

Acknowledgements

Discussions with professor Daniel R. Einstein from Saint Martin's University and with professors J. C. Criscione, K. R. Rajagopal and Arun R. Srinivasa from Texas A&M University are gratefully acknowledged.

References

- [Amensag and McFetridge 2014] S. Amensag and P. S. McFetridge, "Tuning scaffold mechanics by laminating native extracellular matrix membranes and effects on early cellular remodeling", *J. Biomed. Mater. Res. A* **102**:5 (2014), 1325–1333.
- [Becker 1893] G. F. Becker, "The finite elastic stress-strain function", *Am. J. Sci.* **46**:275 (1893), 337–356.
- [Billiar and Sacks 2000a] K. L. Billiar and M. S. Sacks, "Biaxial mechanical properties of the natural and glutaraldehyde treated aortic valve cusp, part I: Experimental results", *J. Biomech. Eng.* **122**:1 (2000), 23–30.
- [Billiar and Sacks 2000b] K. L. Billiar and M. S. Sacks, "Biaxial mechanical properties of the native and glutaraldehyde-treated aortic valve cusp, part II: A structural constitutive model", *J. Biomech. Eng.* **122**:4 (2000), 327–335.
- [Bird et al. 1987a] R. B. Bird, R. C. Armstrong, and O. Hassager, *Dynamics of polymeric liquids, I: Fluid mechanics*, 2nd ed., Wiley, New York, 1987.
- [Bird et al. 1987b] R. B. Bird, C. F. Curtiss, R. C. Armstrong, and O. Hassager, *Dynamics of polymeric liquids, II: Kinetic theory*, 2nd ed., Wiley, New York, 1987.
- [Carathéodory 1909] C. Carathéodory, "Untersuchungen über die Grundlagen der Thermodynamik", *Math. Ann.* **67**:3 (1909), 355–386. Translated in *The second law of thermodynamics* J. Kestin (ed.), Dowden, Hutchinson and Ross, Stroudsburg, PA, (1976) 229–256.
- [Cauchy 1827] A.-L. Cauchy, *Exercices de mathématiques*, de Bure Frères, Paris, 1827.
- [Criscione 2003] J. C. Criscione, "Rivlin's representation formula is ill-conceived for the determination of response functions via biaxial testing", *J. Elasticity* **70**:1-3 (2003), 129–147.
- [Criscione et al. 2000] J. C. Criscione, J. D. Humphrey, A. S. Douglas, and W. C. Hunter, "An invariant basis for natural strain which yields orthogonal stress response terms in isotropic hyperelasticity", *J. Mech. Phys. Solids* **48**:12 (2000), 2445–2465.
- [Criscione et al. 2003a] J. C. Criscione, M. S. Sacks, and W. C. Hunter, "Experimentally tractable, pseudo-elastic constitutive law for biomembranes, I: Theory", *J. Biomech. Eng.* **125**:1 (2003), 94–99.
- [Criscione et al. 2003b] J. C. Criscione, M. S. Sacks, and W. C. Hunter, "Experimentally tractable, pseudo-elastic constitutive law for biomembranes, II: Application", *J. Biomech. Eng.* **125**:1 (2003), 100–105.
- [Dienes 1979] J. K. Dienes, "On the analysis of rotation and stress rate in deforming bodies", *Acta Mech.* **32**:4 (1979), 217–232.
- [Dokos et al. 2002] S. Dokos, B. H. Smaill, A. A. Young, and I. J. LeGrice, "Shear properties of passive ventricular myocardium", *Am. J. Physiol. Heart Circ. Physiol.* **283**:6 (2002), H2650–H2659.
- [Evans and Skalak 1979] E. Evans and R. Skalak, "Mechanics and thermodynamics of biomembranes: part 2", *CRC Crit. Rev. Bioeng.* **3**:4 (1979), 331–418.
- [Freed 2014] A. D. Freed, *Soft solids: a primer to the theoretical mechanics of materials*, Birkhäuser, Basel, 2014.
- [Freed and Rajagopal 2016] A. D. Freed and K. R. Rajagopal, "A promising approach for modeling biological fibers", *Acta Mech.* **227**:6 (2016), 1609–1619.

- [Freed and Srinivasa 2015] A. D. Freed and A. R. Srinivasa, “Logarithmic strain and its material derivative for a QR decomposition of the deformation gradient”, *Acta Mech.* **226**:8 (2015), 2645–2670.
- [Freed, Liao and Einstein 2014] A. D. Freed, J. Liao, and D. R. Einstein, “A membrane model form implicit elasticity theory: application to visceral pleura”, *Biomech. Model. Mechanobiol.* **13**:4 (2014), 871–881.
- [Fung 1993] Y. C. Fung, *Biomechanics: mechanical properties of living tissues*, 2nd ed., Springer, New York, 1993.
- [Grashow et al. 2006] J. S. Grashow, A. P. Yoganathan, and M. S. Sacks, “Biaxial stress–stretch behavior of the mitral valve anterior leaflet at physiologic strain rates”, *Ann. Biomed. Eng.* **34**:2 (2006), 315–325.
- [Green 1848] G. Green, “On the propagation of light in crystallized media”, *Trans. Cambridge Philos. Soc.* **7** (1848), 121–140.
- [Green and Naghdi 1965] A. E. Green and P. M. Naghdi, “A general theory of an elastic-plastic continuum”, *Arch. Rational Mech. Anal.* **18**:4 (1965), 251–281.
- [Helfrich 1973] W. Helfrich, “Elastic properties of lipid bilayers: theory and possible experiments”, *Z. Naturforsch. C.* **28**:11 (1973), 693–703.
- [Hill 1978] R. Hill, *Aspects of invariance in solid mechanics*, Advances in applied mechanics **18**, Academic Press, New York, 1978.
- [Humphrey 1998] J. Humphrey, “Computer methods in membrane biomechanics”, *Comput. Methods Biomech. Biomed. Eng.* **1**:3 (1998), 171–210.
- [Humphrey et al. 1987] J. Humphrey, D. Vawter, and R. Vito, “Quantification of strains in biaxially tested soft tissues”, *J. Biomech.* **20**:1 (1987), 59–65.
- [Kestin and Rice 1970] J. Kestin and J. R. Rice, “Paradoxes in the application of thermodynamics to strained solids”, pp. 275–298 in *A critical review of thermodynamics*, edited by E. Stuart et al., Mono Book Corp., Baltimore, MD, 1970.
- [Kharaziha et al. 2013] M. Kharaziha, M. Nikkhah, S.-R. Shin, N. Annabi, N. Mosoumi, A. Gaharwar, G. Camci-Unal, and A. Khademhosseini, “PGS: gelatin nanofibrous scaffolds with tunable mechanical and structural properties for engineering cardiac tissues”, *Biomaterials* **34**:27 (2013), 6355–6366.
- [Kirchhoff 1852] G. Kirchhoff, “Über die Gleichungen des Gleichgewichtes eines elastischen Körpers bei nicht unendlich kleinen Verschiebungen seiner Theile”, *Sitzungsberichte der Akademie der Wissenschaften, Wien* **9** (1852), 763–773.
- [Lanir and Fung 1974] Y. Lanir and Y. Fung, “Two-dimensional mechanical properties of rabbit skin, I: Experimental system”, *J. Biomech.* **7**:1 (1974), 29–34.
- [Lodge 1964] A. Lodge, *Elastic liquids: an introductory vector treatment of finite-strain polymer rheology*, Academic Press, London, 1964.
- [Lodge 1974] A. Lodge, *Body tensor fields in continuum mechanics: with applications to polymer rheology*, Academic Press, New York, 1974.
- [Lubarda 2010] V. A. Lubarda, “Constitutive analysis of thin biological membranes with application to radial stretching of a hollow circular membrane”, *J. Mech. Phys. Solids* **58**:6 (2010), 860–873.
- [Murnaghan 1954] F. D. Murnaghan, “On the unitary invariants of a square matrix”, *Anais Acad. Brasil. Ci.* **26** (1954), 1–7.
- [Noll 1955] W. Noll, “On the continuity of the solid and fluid states”, *J. Rational Mech. Anal.* **4** (1955), 3–81.
- [Ogden 1984] R. Ogden, *Non-linear elastic deformations*, Wiley, New York, 1984.
- [Oldroyd 1950] J. G. Oldroyd, “On the formulation of rheological equations of state”, *Proc. Roy. Soc. London. A.* **200** (1950), 523–541.
- [Pipkin 1986] A. C. Pipkin, “The relaxed energy density for isotropic elastic membranes”, *IMA J. Appl. Math.* **36**:1 (1986), 85–99.
- [Poynting 1909] J. H. Poynting, “On pressure perpendicular to the shear planes in finite pure shears, and on the lengthening of loaded wires when twisted”, *Proc. Roy. Soc. London. A.* **82**:557 (1909), 546–559.
- [Rajagopal 2003] K. R. Rajagopal, “On implicit constitutive theories”, *Appl. Math.* **48**:4 (2003), 279–319.
- [Rajagopal 2011] K. R. Rajagopal, “Conspectus of concepts of elasticity”, *Math. Mech. Solids* **16**:5 (2011), 536–562.
- [Rivlin and Smith 1969] R. Rivlin and G. Smith, “Orthogonal integrity basis for N symmetric matrices”, pp. 121–141 in *Contributions to mechanics*, edited by D. Abir, Pergamon Press, New York, 1969.

- [Rosakis 1990] P. Rosakis, “Ellipticity and deformations with discontinuous gradients in finite elastostatics”, *Arch. Rational Mech. Anal.* **109**:1 (1990), 1–37.
- [Sacks 1999] M. Sacks, “A method for planar biaxial mechanical testing that includes in-plane shear”, *J. Biomech. Eng.* **121**:5 (1999), 551–555.
- [Sacks 2000] M. S. Sacks, “Biaxial mechanical evaluation of planar biological materials”, *J. Elasticity* **61**:1-3 (2000), 199–246.
- [Sacks and Chuong 1993] M. Sacks and C. Chuong, “Biaxial mechanical properties of passive right ventricular free wall myocardium”, *J. Biomech. Eng.* **115**:2 (1993), 202–205.
- [Simo and Hughes 1998] J. C. Simo and T. J. R. Hughes, *Computational inelasticity*, Interdisciplinary Applied Mathematics **7**, Springer, New York, 1998.
- [Spencer 1972] A. Spencer, *Deformations in fibre-reinforced materials*, Clarendon Press, Oxford, England, 1972.
- [Srinivasa 2012] A. R. Srinivasa, “On the use of the upper triangular (or QR) decomposition for developing constitutive equations for Green-elastic materials”, *Int. J. Eng. Sci.* **60** (2012), 1–12.
- [Steigmann 1990] D. J. Steigmann, “Tension-field theory”, *Proc. Roy. Soc. London A* **429**:1876 (1990), 141–173.
- [Stewart 1973] G. W. Stewart, *Introduction to matrix computations*, Academic Press, New York, 1973.
- [Thomson 1878] W. Thomson, “On the thermoelastic, thermomagnetic, and pyroelectric properties of matter”, *Philos. Mag.* **5**:28 (1878), 4–27.
- [Ting 1985] T. C. T. Ting, “Determination of $\mathbf{C}^{1/2}$, $\mathbf{C}^{-1/2}$ and more general tensor functions of \mathbf{C} ”, *J. Elasticity* **15**:3 (1985), 319–323.
- [Truesdell and Noll 2004] C. Truesdell and W. Noll, *The non-linear field theories of mechanics*, 3rd ed., Springer, Berlin, 2004.
- [Xie et al. 2015] M. Xie, J. Ge, Y. Xue, Y. Du, B. Lei, and P. X. Ma, “Photo-crosslinked fabrication of novel biocompatible and elastomeric star-shaped inositol-based polymer with highly tunable mechanical behavior and degradation”, *J. Mech. Behav. Biomed. Mater.* **51** (2015), 163–168.

Received 22 Jul 2016. Revised 2 Oct 2016. Accepted 18 Oct 2016.

ALAN D. FREED: afreed@tamu.edu

Department of Mechanical Engineering, Texas A&M University, TAMU 3123, College Station, TX 77843, United States

VEYSEL EREL: veyselere1@hotmail.com

Department of Mechanical Engineering, Texas A&M University, TAMU 3123, College Station, TX 77843, United States

MICHAEL R. MORENO: michael.moreno@tamu.edu

Department of Mechanical Engineering, Texas A&M University, TAMU 3123, College Station, TX 77843, United States

JOURNAL OF MECHANICS OF MATERIALS AND STRUCTURES

msp.org/jomms

Founded by Charles R. Steele and Marie-Louise Steele

EDITORIAL BOARD

| | |
|-----------------------|--|
| ADAIR R. AGUIAR | University of São Paulo at São Carlos, Brazil |
| KATIA BERTOLDI | Harvard University, USA |
| DAVIDE BIGONI | University of Trento, Italy |
| YIBIN FU | Keele University, UK |
| IWONA JASIUK | University of Illinois at Urbana-Champaign, USA |
| C. W. LIM | City University of Hong Kong |
| THOMAS J. PENCE | Michigan State University, USA |
| GIANNI ROYER-CARFAGNI | Università degli studi di Parma, Italy |
| DAVID STEIGMANN | University of California at Berkeley, USA |
| PAUL STEINMANN | Friedrich-Alexander-Universität Erlangen-Nürnberg, Germany |

ADVISORY BOARD

| | |
|---------------|---|
| J. P. CARTER | University of Sydney, Australia |
| D. H. HODGES | Georgia Institute of Technology, USA |
| J. HUTCHINSON | Harvard University, USA |
| D. PAMPLONA | Universidade Católica do Rio de Janeiro, Brazil |
| M. B. RUBIN | Technion, Haifa, Israel |

PRODUCTION production@msp.org

SILVIO LEVY Scientific Editor


Cover photo: Mando Gomez, www.mandolux.com

See msp.org/jomms for submission guidelines.

JoMMS (ISSN 1559-3959) at Mathematical Sciences Publishers, 798 Evans Hall #6840, c/o University of California, Berkeley, CA 94720-3840, is published in 10 issues a year. The subscription price for 2017 is US \$615/year for the electronic version, and \$775/year (+\$60, if shipping outside the US) for print and electronic. Subscriptions, requests for back issues, and changes of address should be sent to MSP.

JoMMS peer-review and production is managed by EditFlow[®] from Mathematical Sciences Publishers.

PUBLISHED BY

 **mathematical sciences publishers**
nonprofit scientific publishing

<http://msp.org/>

© 2017 Mathematical Sciences Publishers

Journal of Mechanics of Materials and Structures

Volume 12, No. 2

March 2017

- A note on cross product between two symmetric second-order tensors**
LÁSZLÓ SZABÓ 147
- Fracture in three dimensions due to die motion on crack surfaces: framework for study of crack/contact zone geometry**
LOUIS M. BROCK 159
- Maxwell's equivalent inhomogeneity and remarkable properties of harmonic problems involving symmetric domains**
SOFIA G. MOGILEVSKAYA and DMITRY NIKOLSKIY 179
- Interfacial microscopic boundary conditions associated with backstress-based higher-order gradient crystal plasticity theory**
MITSUTOSHI KURODA 193
- Conjugate stress/strain base pairs for planar analysis of biological tissues**
ALAN D. FREED, VEYSEL EREL and MICHAEL R. MORENO 219